HIGHT LIFT DEVICES

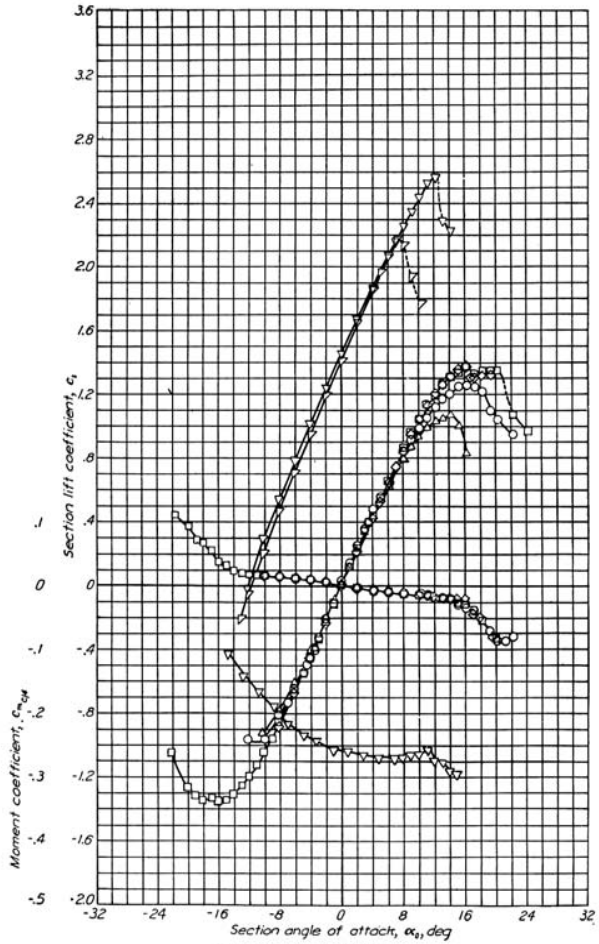

NACA 65$_3$-018 Wing Section

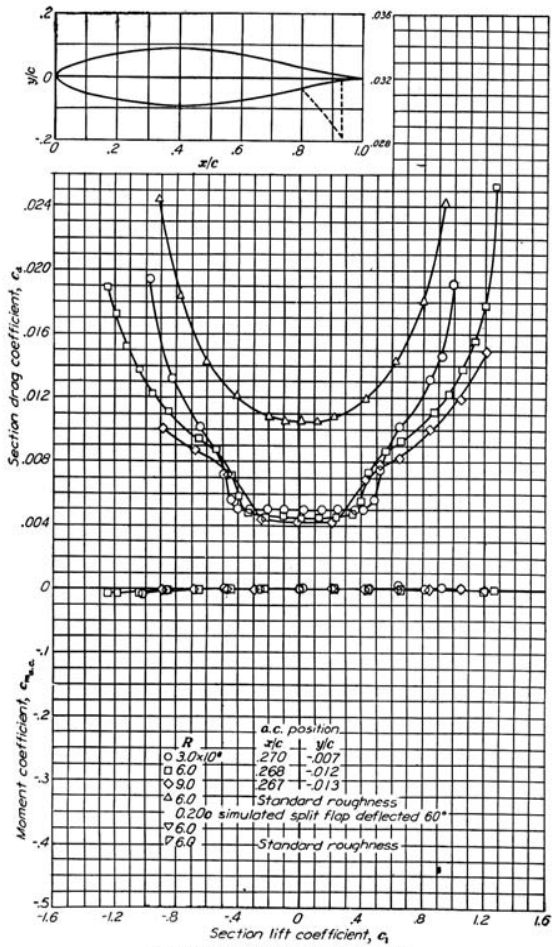

NACA 65$_3$-018 Wing Section (*Continued*)

HIGHT LIFT DEVICES

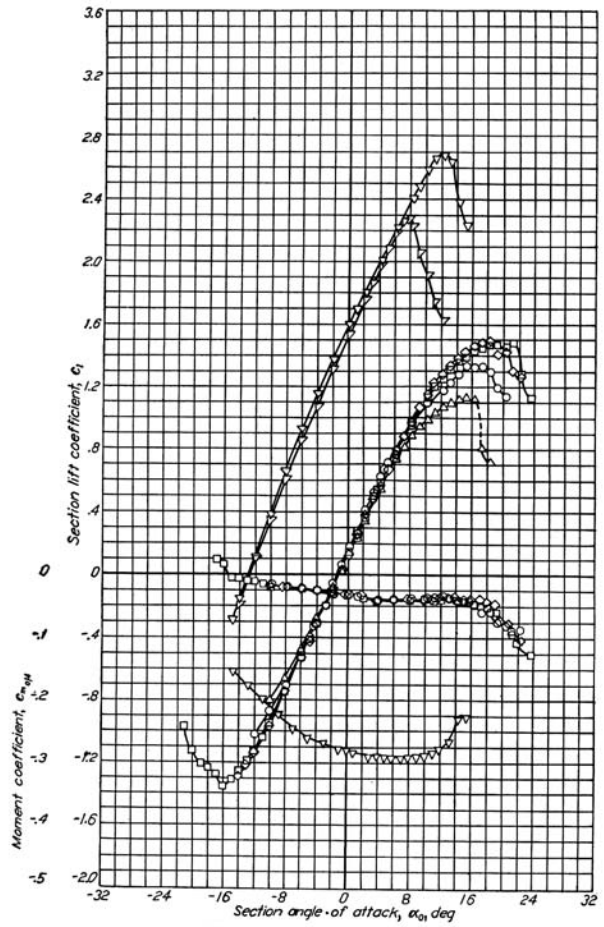

NACA 65$_3$-218 Wing Section

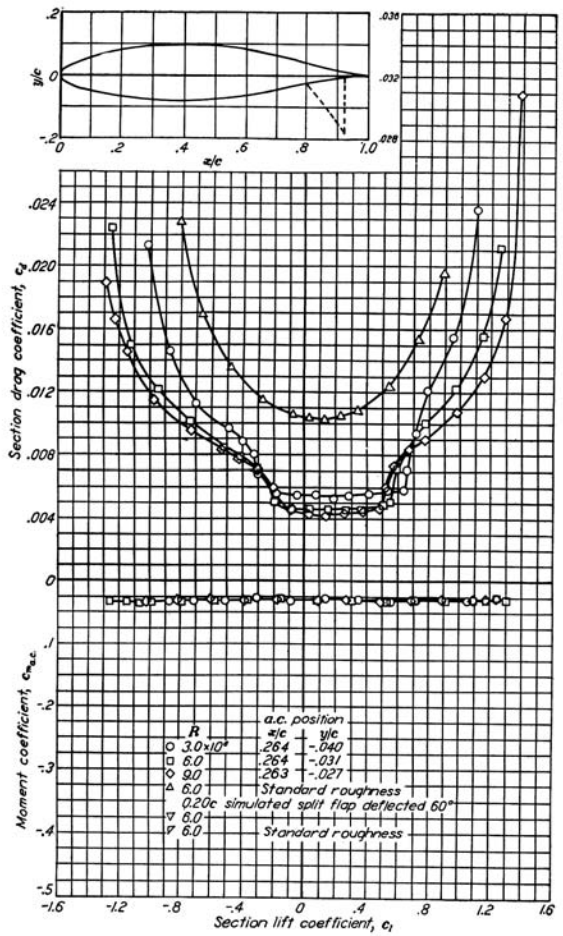

NACA 65$_3$-218 Wing Section (*Continued*)

HIGHT LIFT DEVICES

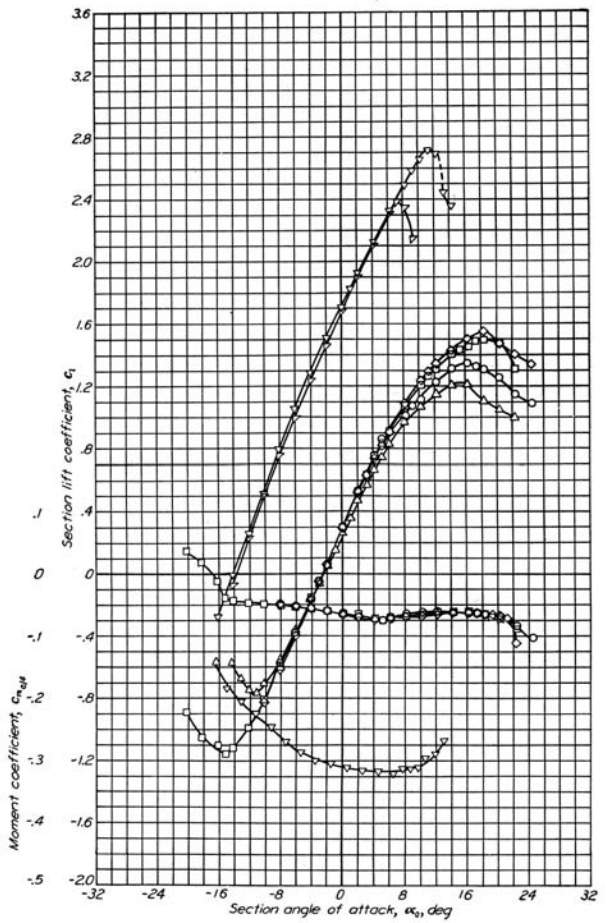

NACA 65₂-418 Wing Section

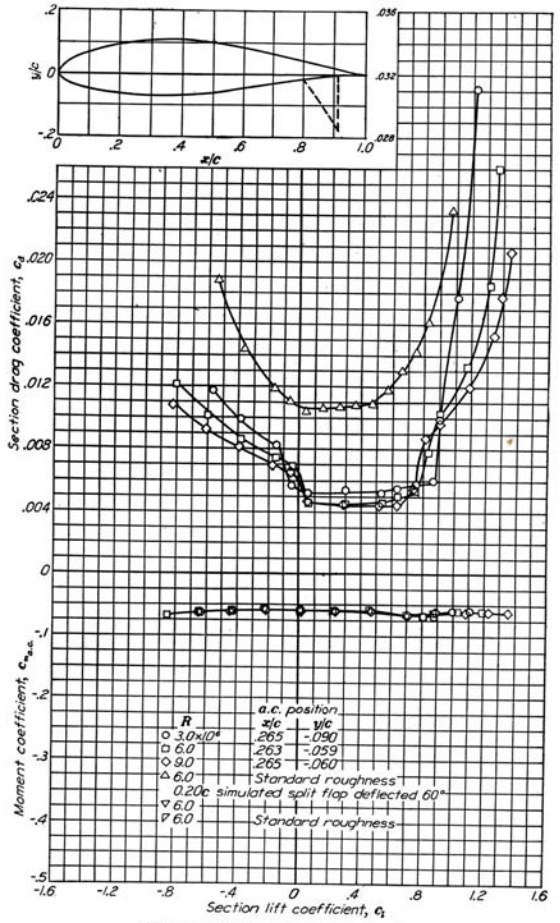

NACA 65₂-418 Wing Section (*Continued*)

HIGHT LIFT DEVICES

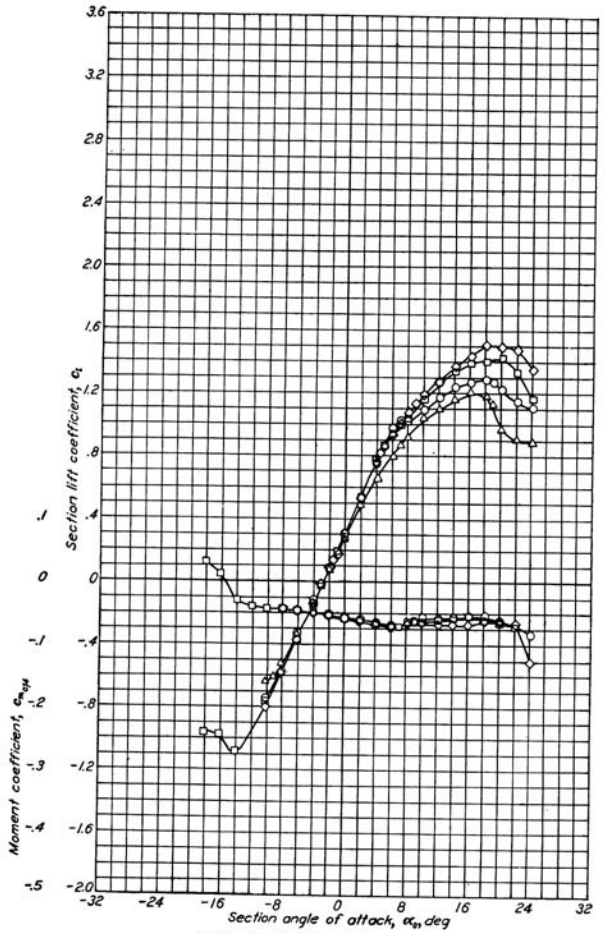

NACA 65$_1$-418 Wing Section
$a = 0.5$

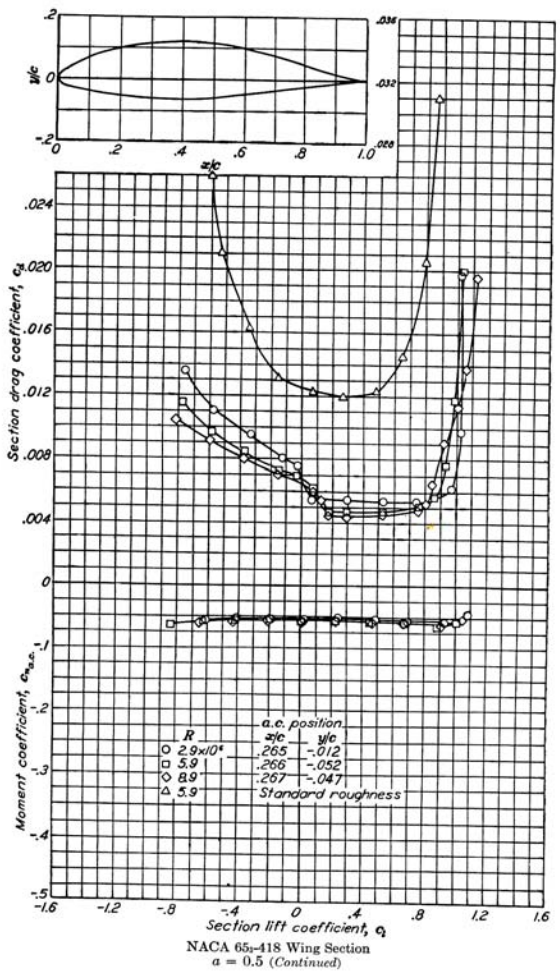

NACA 65$_1$-418 Wing Section
$a = 0.5$ *(Continued)*

HIGHT LIFT DEVICES

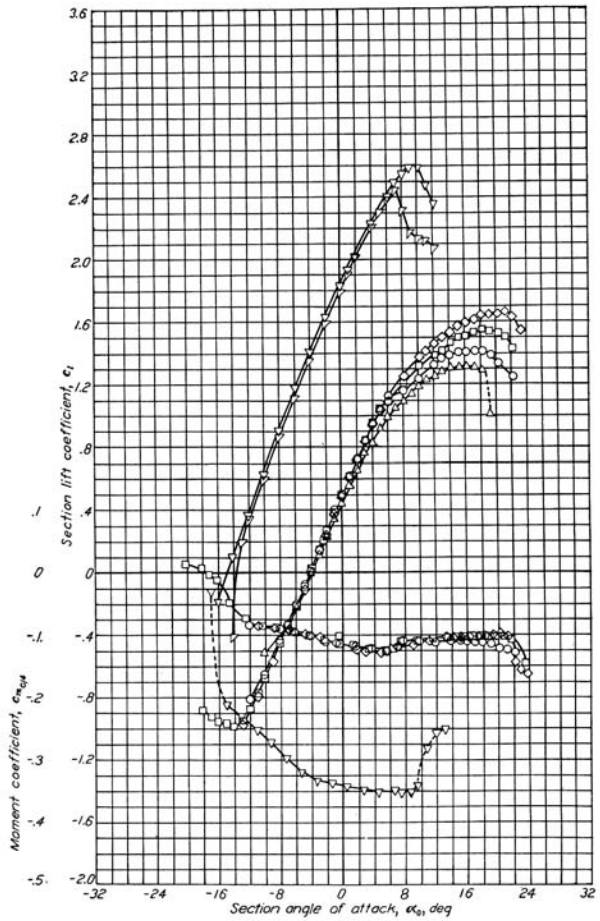

NACA 65_2-618 Wing Section

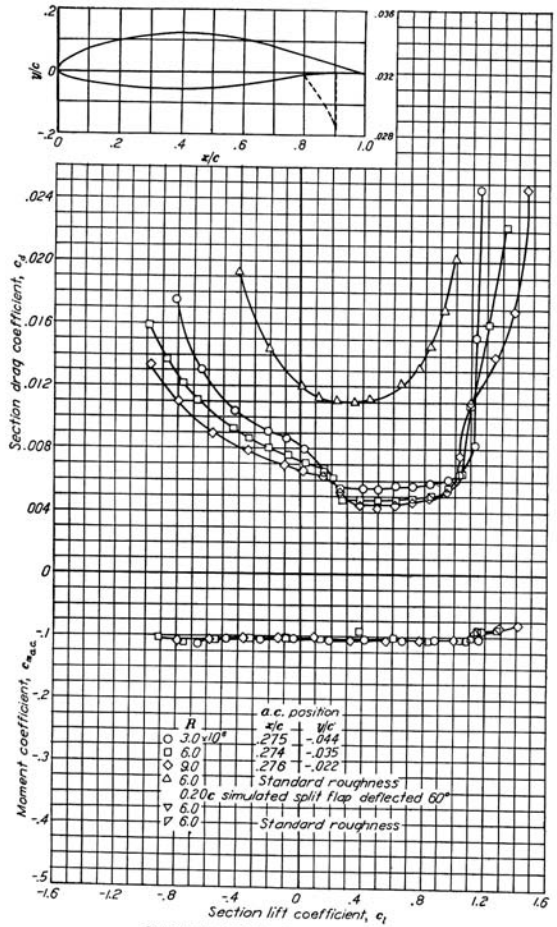

NACA 65_2-618 Wing Section (*Continued*)

HIGHT LIFT DEVICES

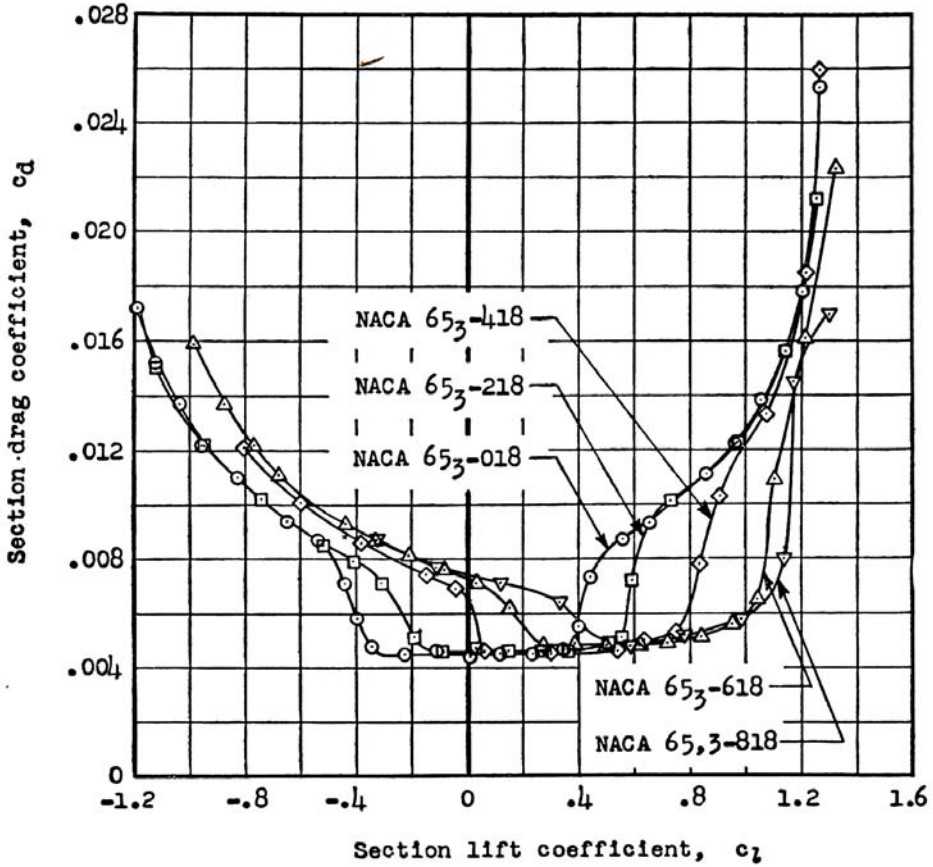

FIG. 71. Drag characteristics of some NACA 65-series airfoil sections of 18 per cent thickness with various amounts of camber. R, 6×10^6.

HIGHT LIFT DEVICES

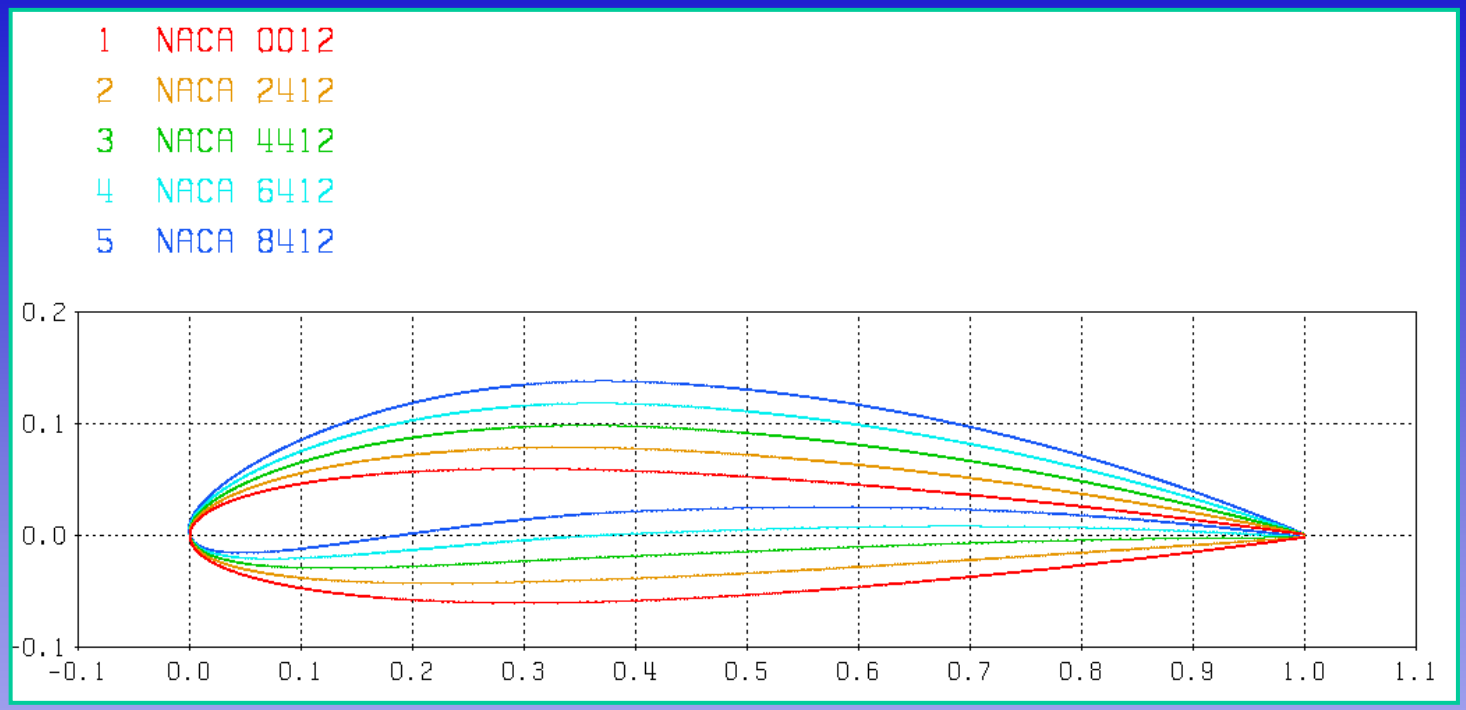

HIGHT LIFT DEVICES

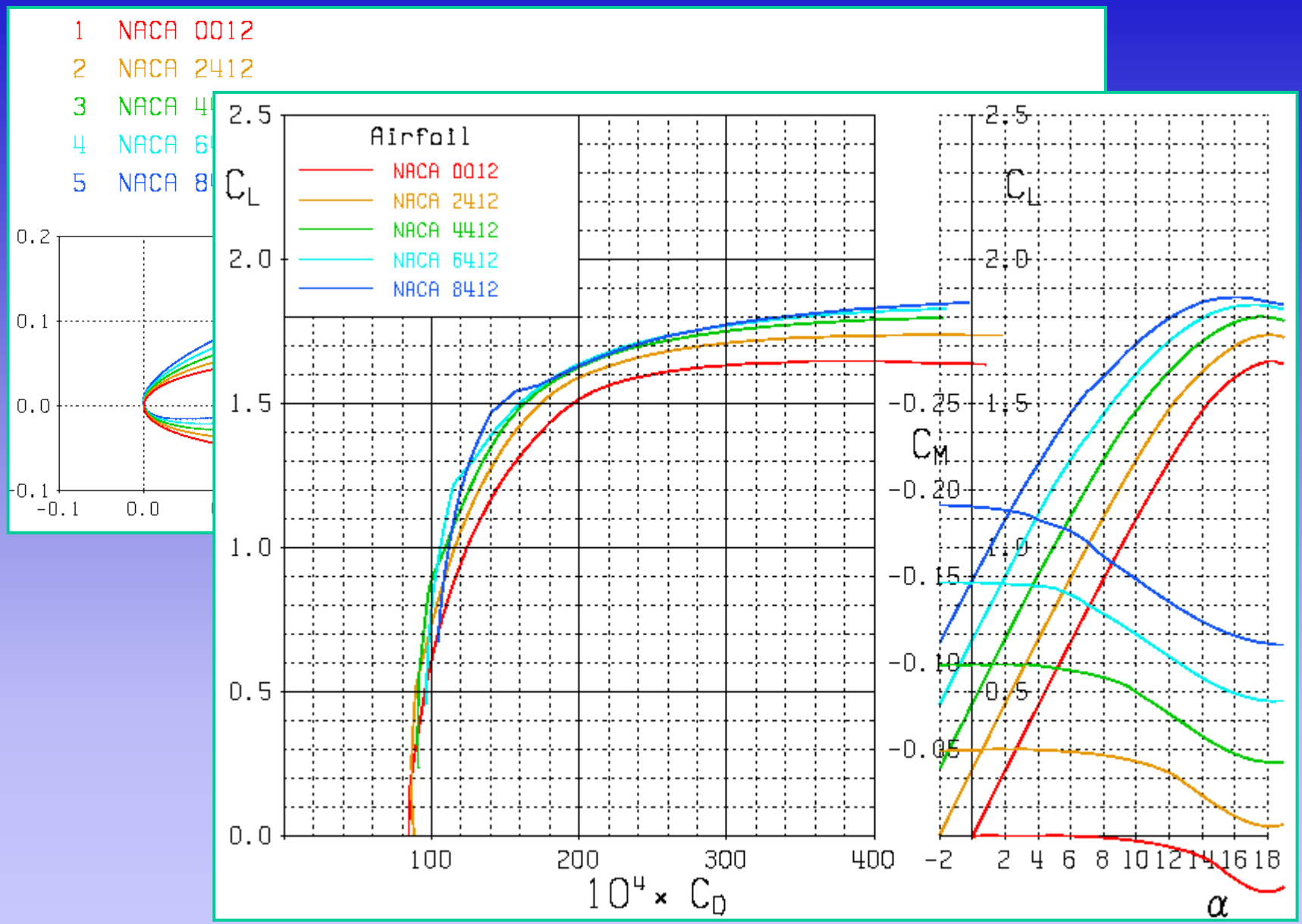

HIGHT LIFT DEVICES

$CL_{MAX} \div CL_{OPT} \div CL_{MIN}$

CD_{MIN}

α

HIGHT LIFT DEVICES

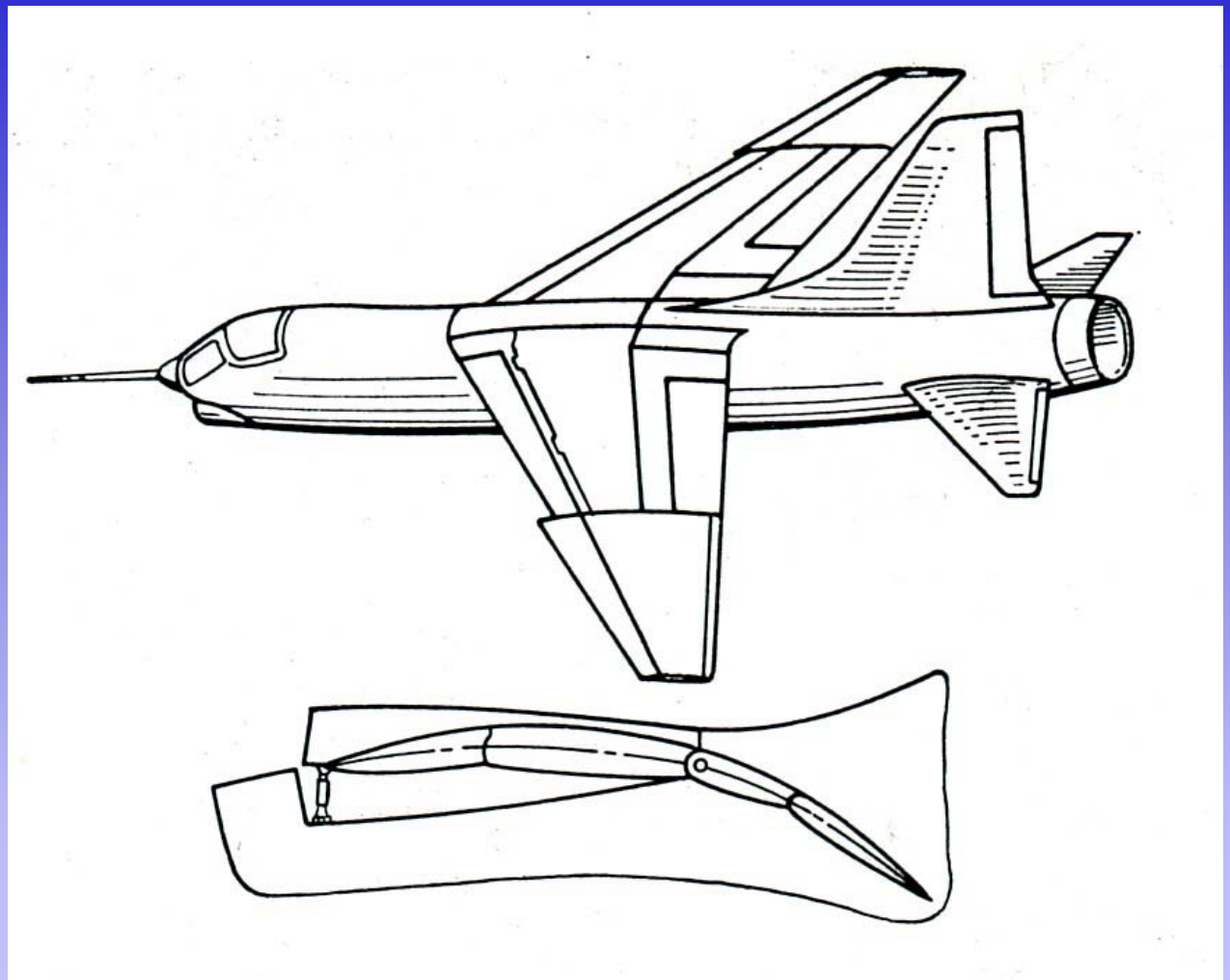

HIGHT LIFT DEVICES

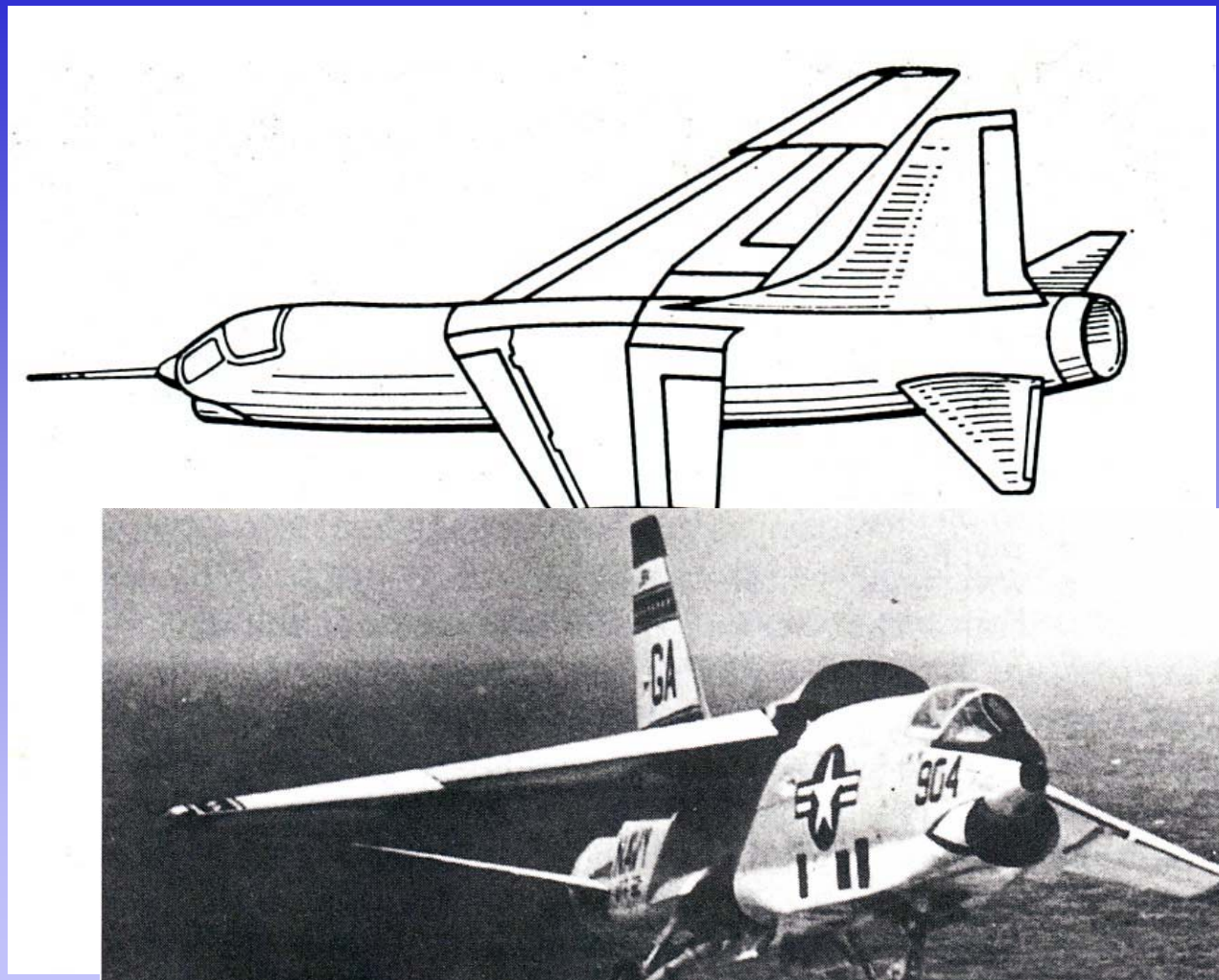

HIGHT LIFT DEVICES

F-5E

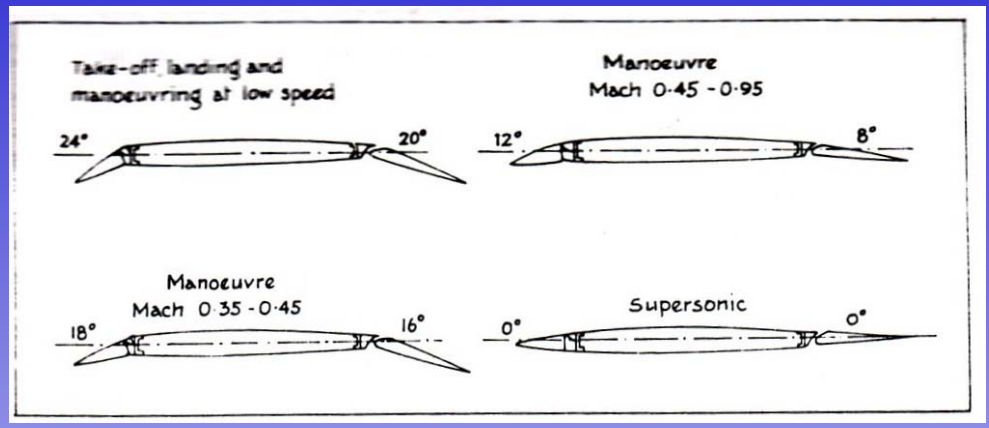

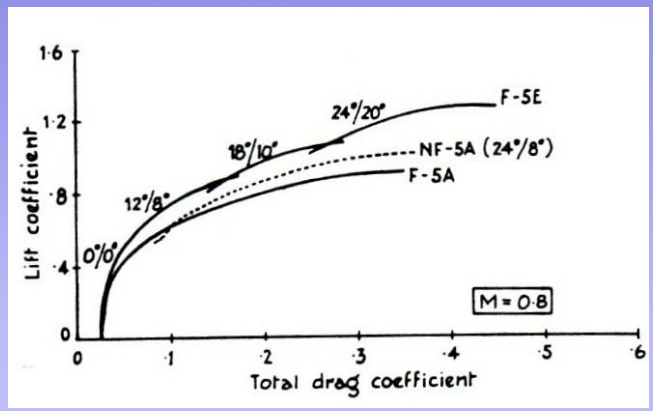

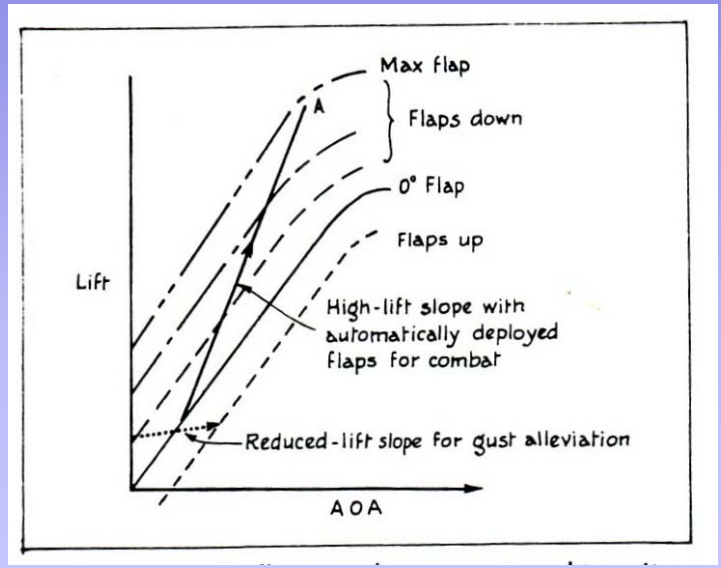

HIGHT LIFT DEVICES

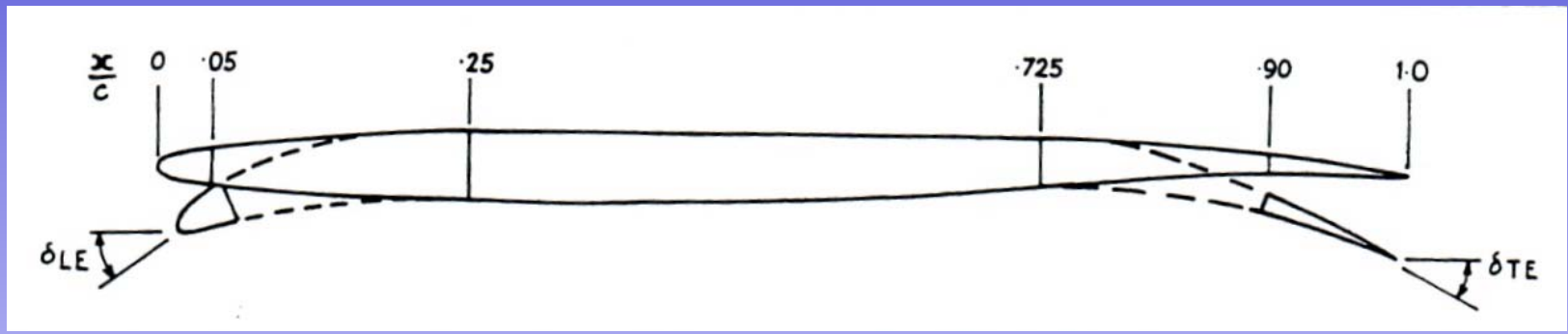

HIGHT LIFT DEVICES

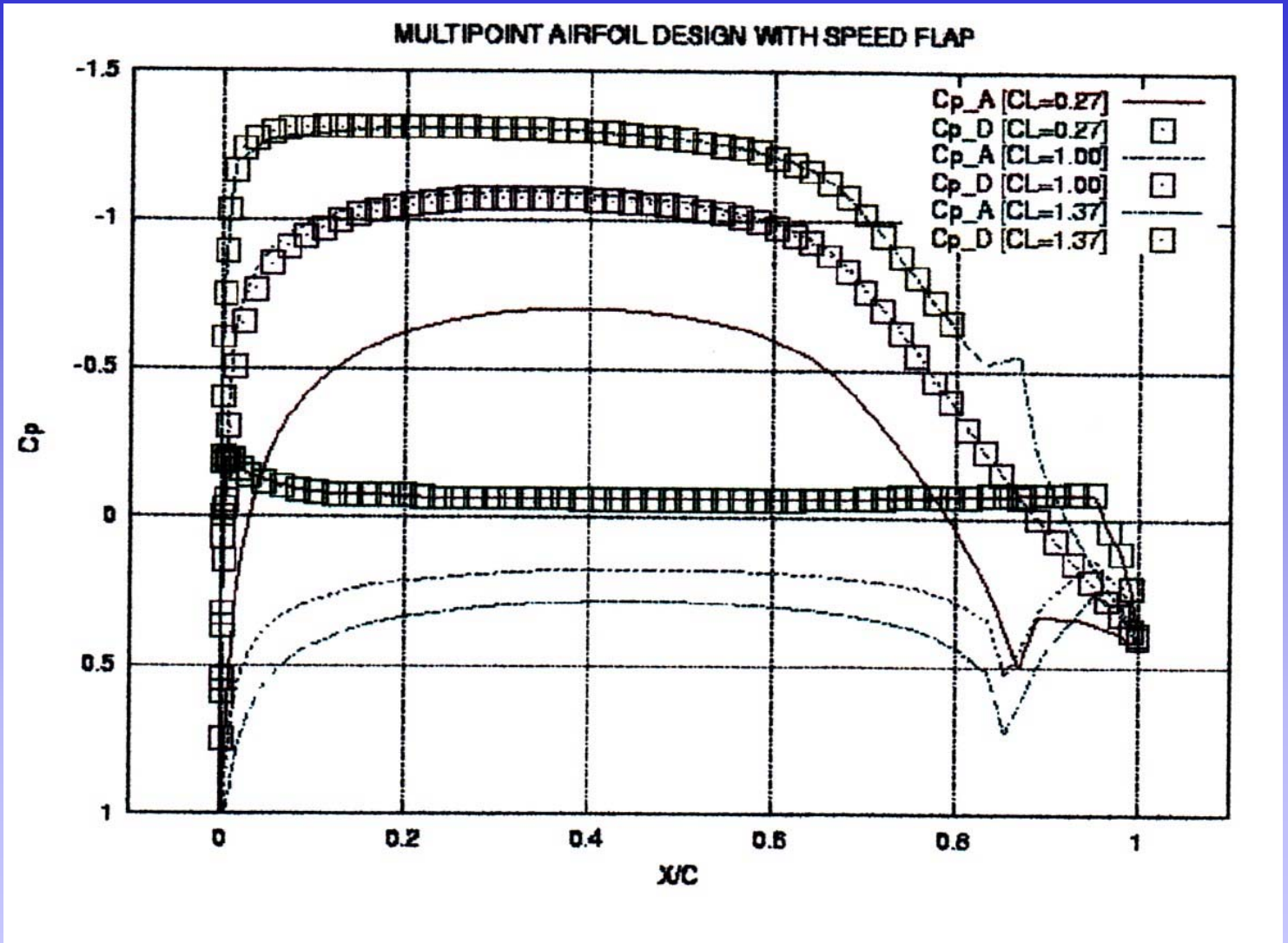

HIGHT LIFT DEVICES

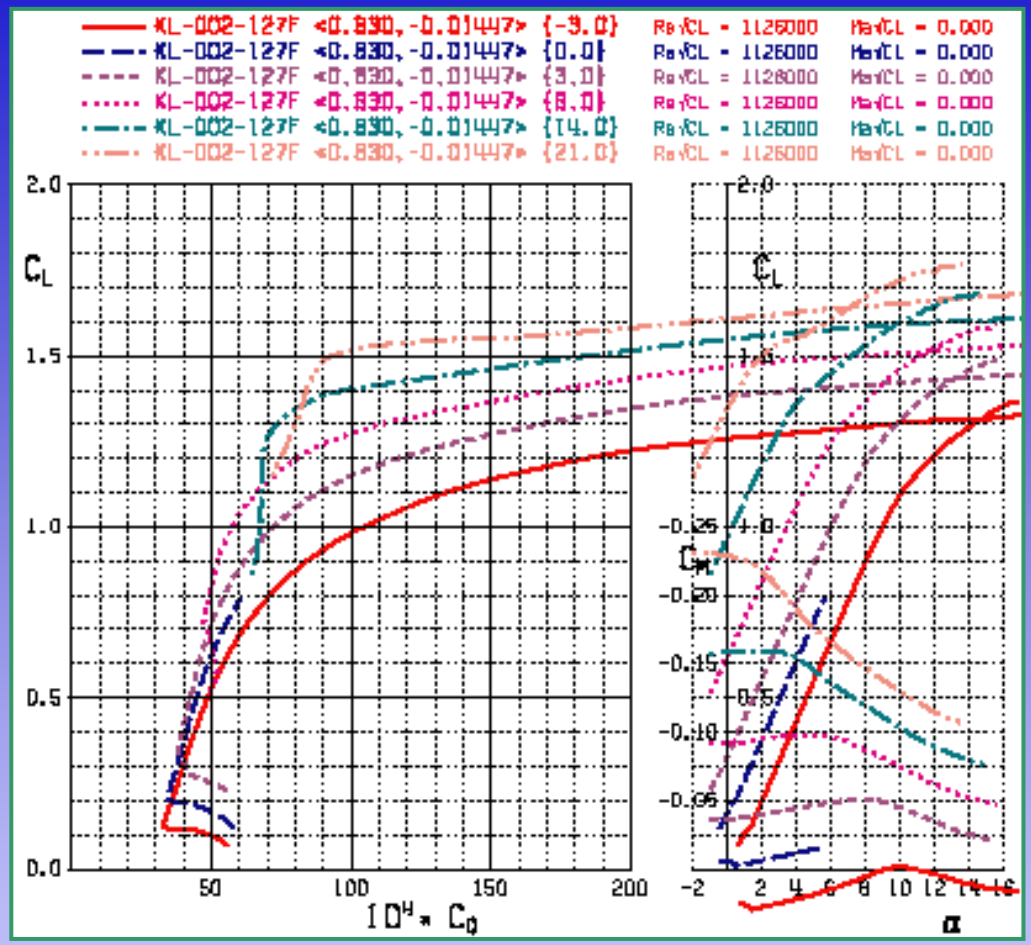

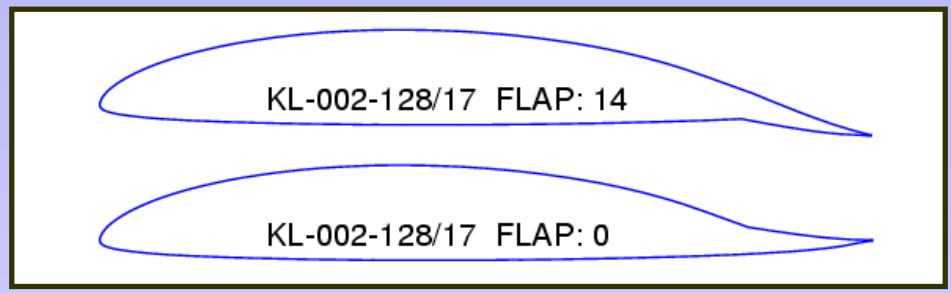

CL_{MAX} V_{MIN} α_{CR}

Thin Airfoil Theory (Glauert)

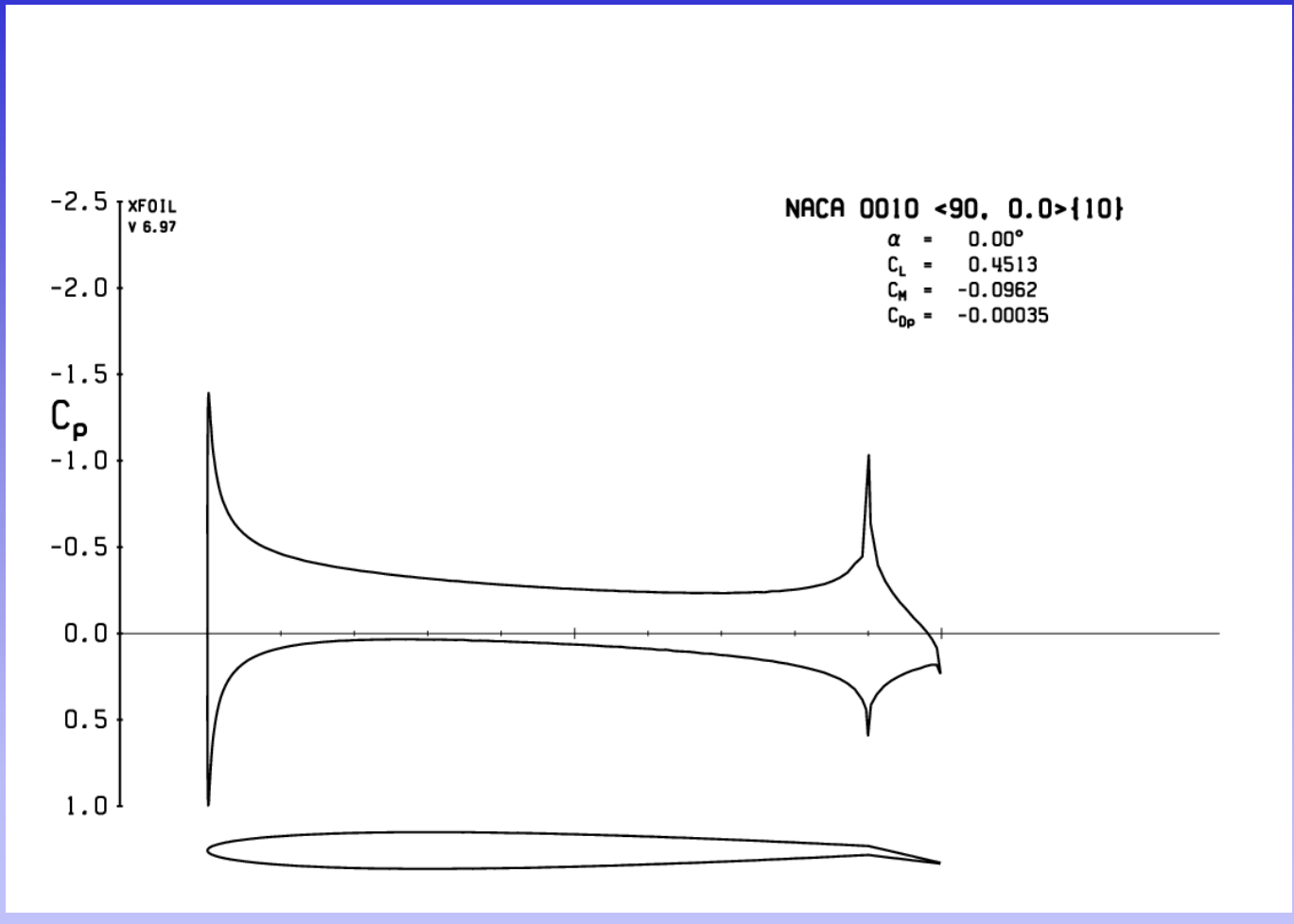

Thin Airfoil Theory (Glauert)

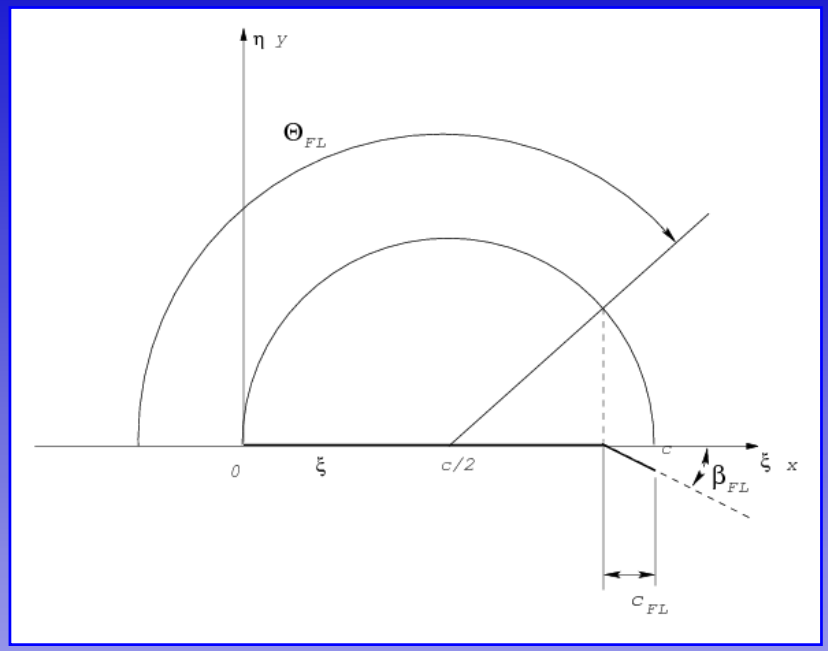

$$C_L = 2\pi \cdot \left(A_0 + \frac{1}{2} A_1 \right) \approx$$

$$2\pi \cdot \left(\alpha + \underbrace{\frac{4\sqrt{\bar{c}_{FL}}}{\pi} \cdot \beta_{FL}}_{-\alpha_0} \right) = \underbrace{2\pi \cdot \alpha + 8\sqrt{\bar{c}_{FL}} \cdot \beta_{FL}}_{C_{L_0}}$$

Thin Airfoil Theory (Glauert)

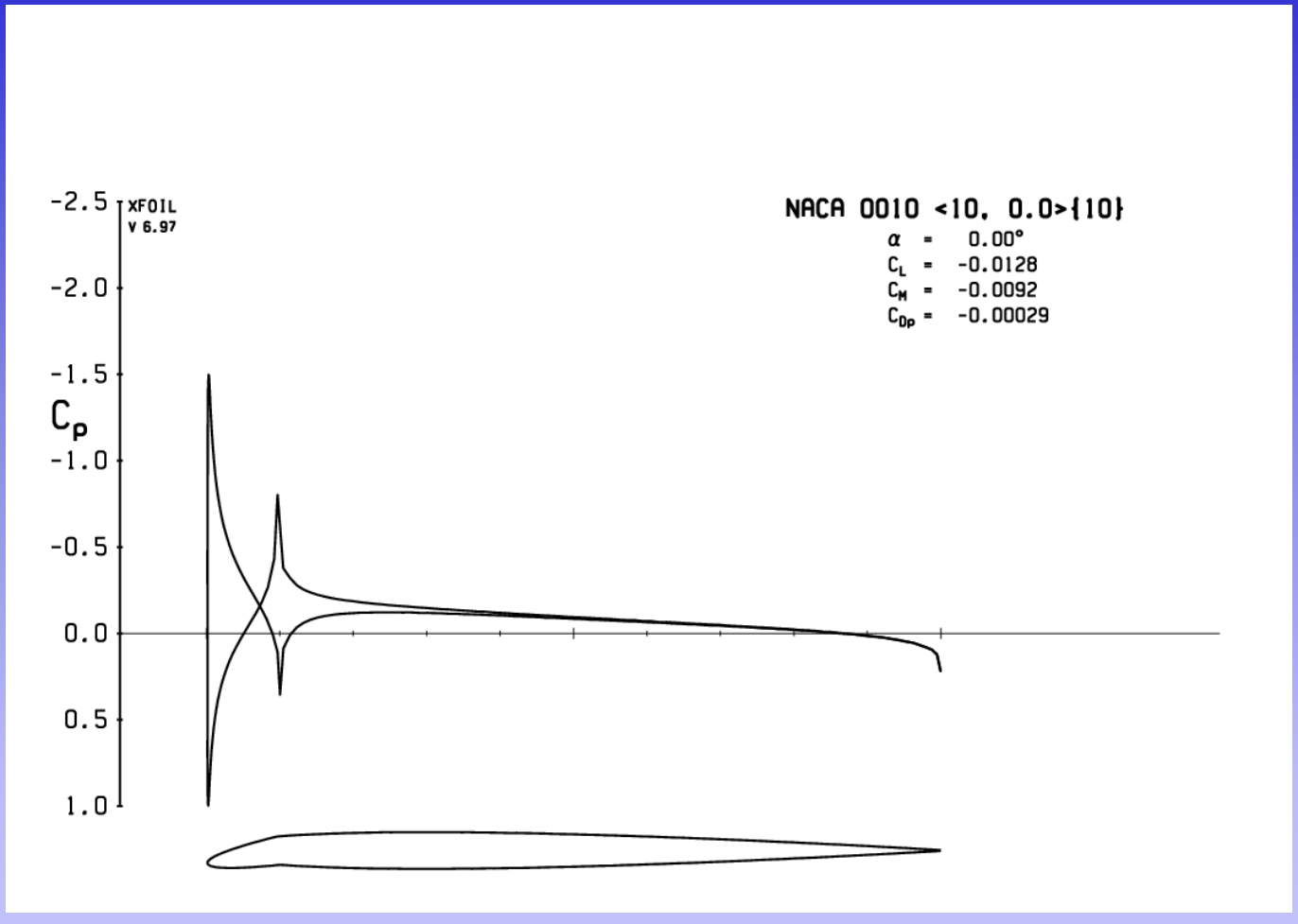

Thin Airfoil Theory (Glauert)

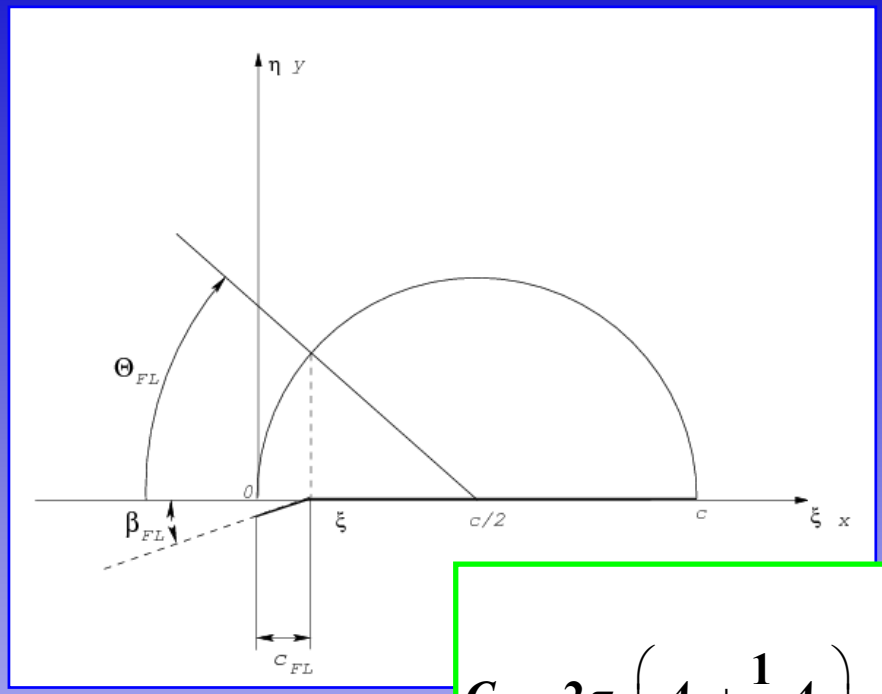

$$C_L = 2\pi \cdot \left(A_0 + \frac{1}{2} A_1 \right) =$$

$$\approx 2\pi \cdot \left(\alpha \overbrace{- \left(\frac{4}{3\pi} \cdot \bar{c}_{FL}^{3/2} - \ldots \right) \cdot \beta_{FL}}^{-\alpha_0} \right) =$$

$$2\pi \cdot \alpha \underbrace{- \left(\frac{8}{3} \cdot \bar{c}_{FL}^{3/2} - \ldots \right) \cdot \beta_{FL}}_{CL_0} \approx \quad 2\pi \cdot \alpha$$

Thin Airfoil Theory (Glauert)

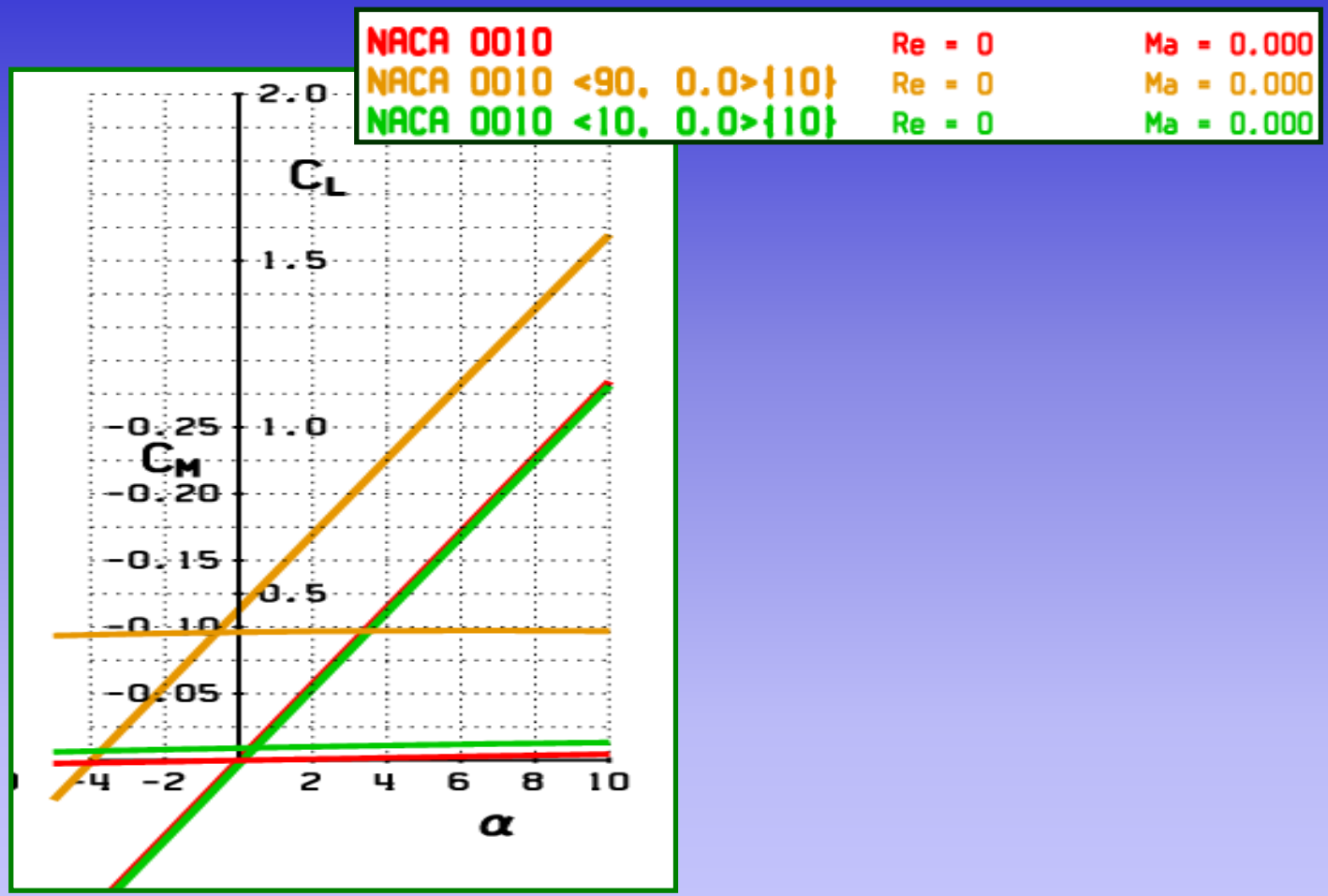

HIGHT LIFT DEVICES

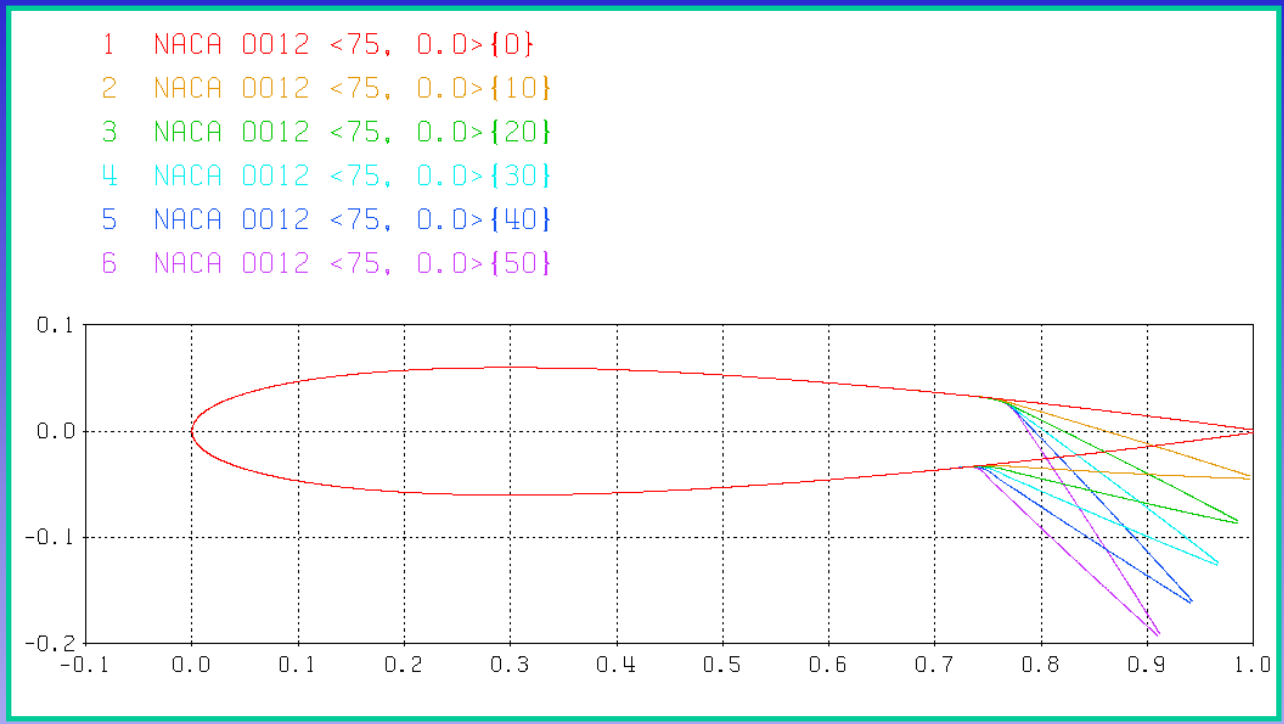

HIGHT LIFT DEVICES

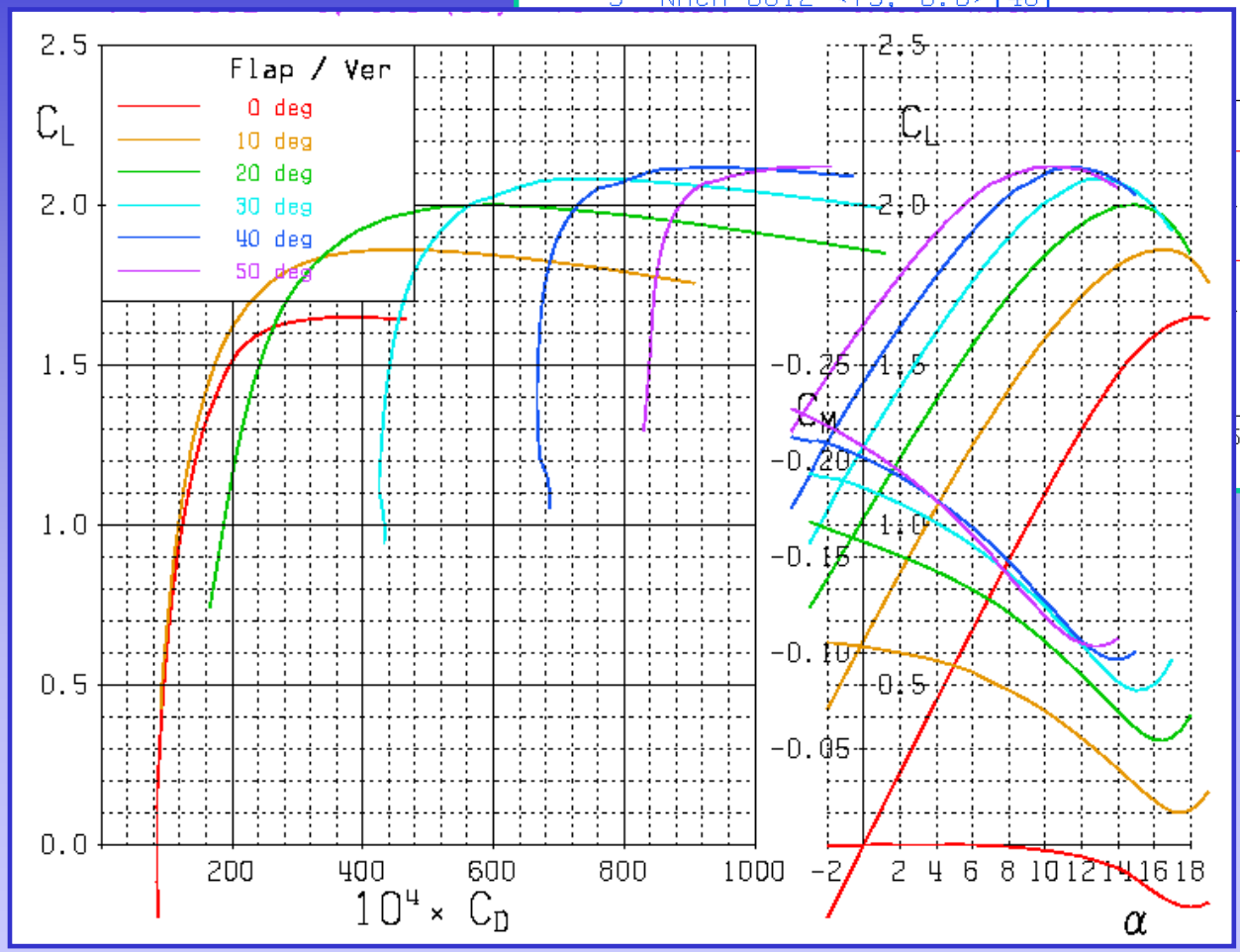

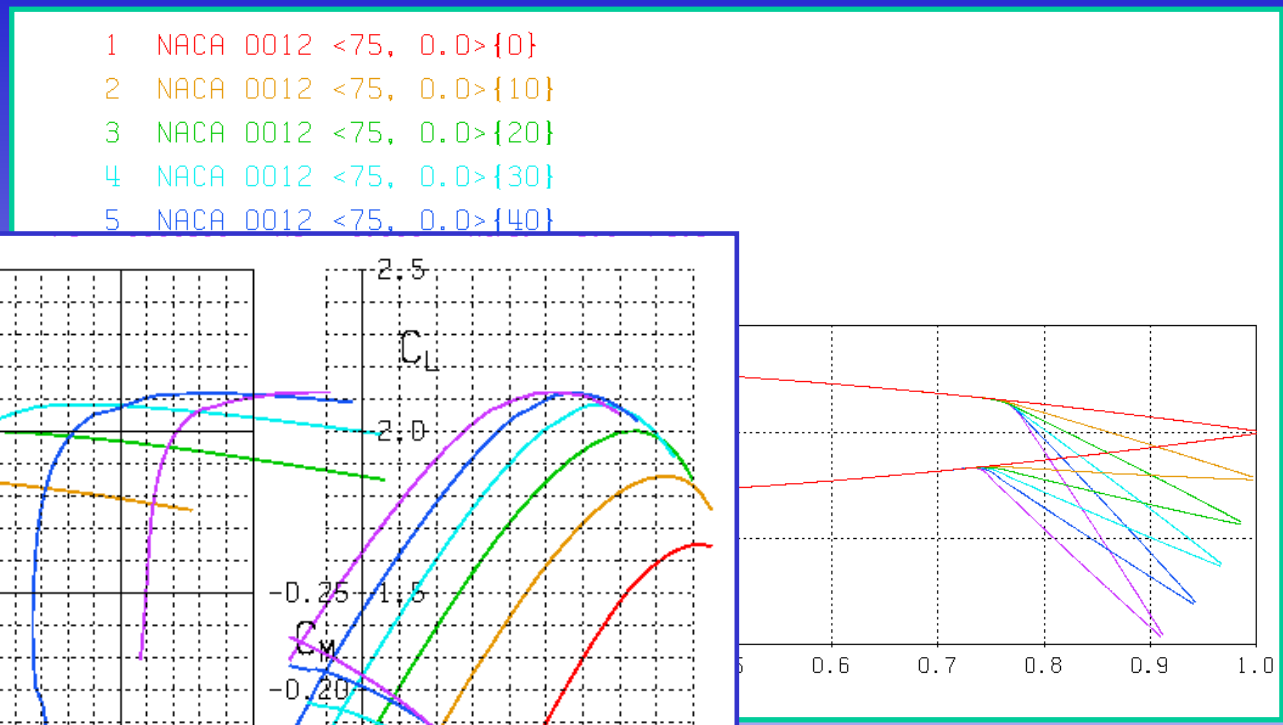

HIGHT LIFT DEVICES

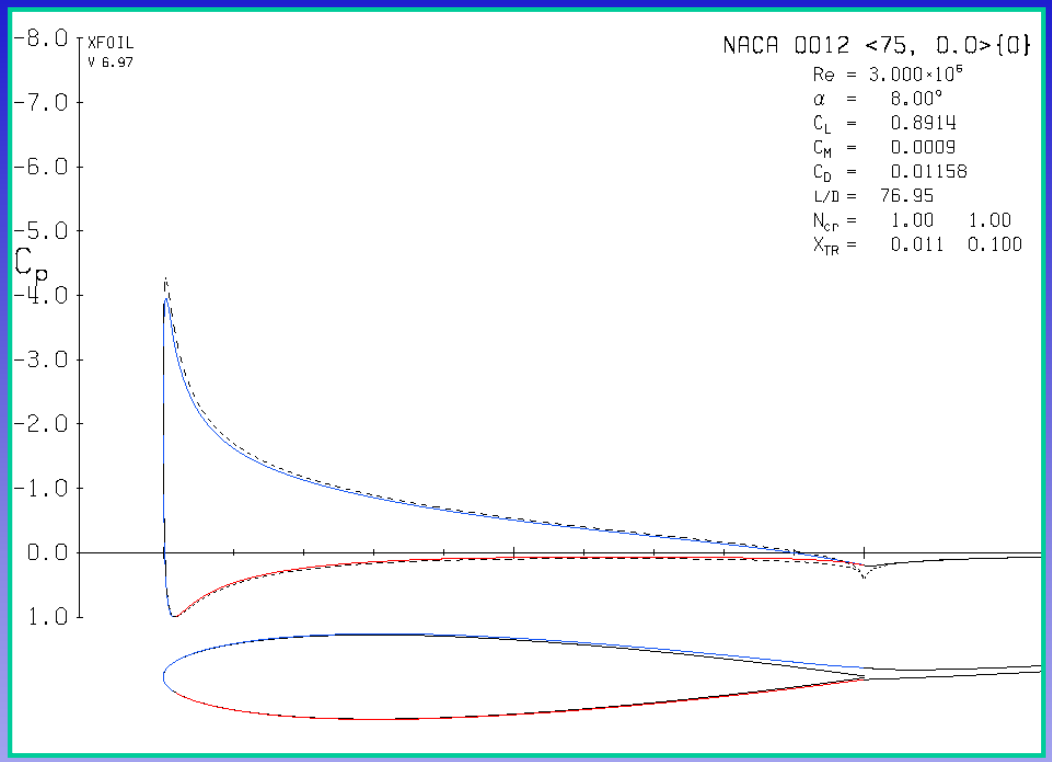

HIGHT LIFT DEVICES

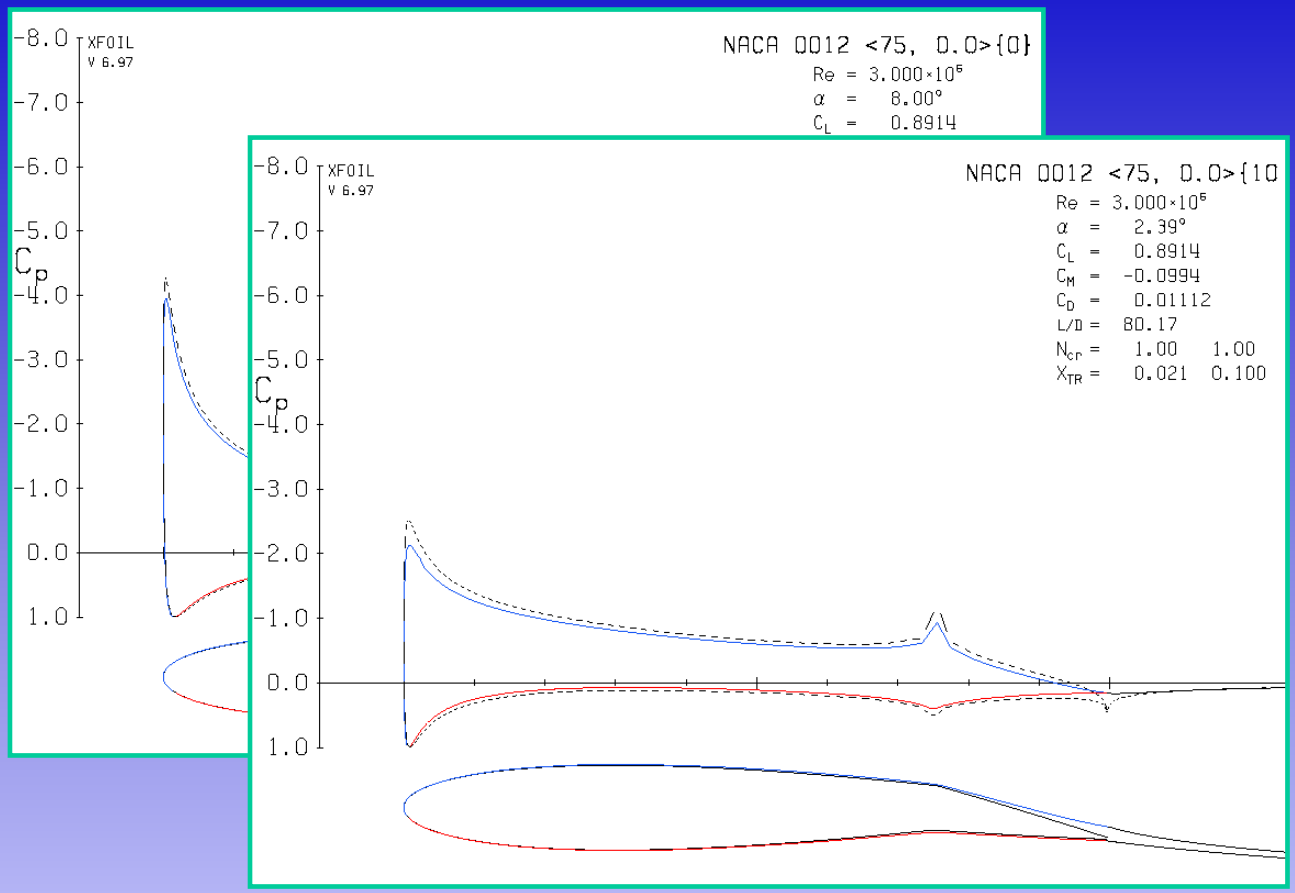

HIGHT LIFT DEVICES

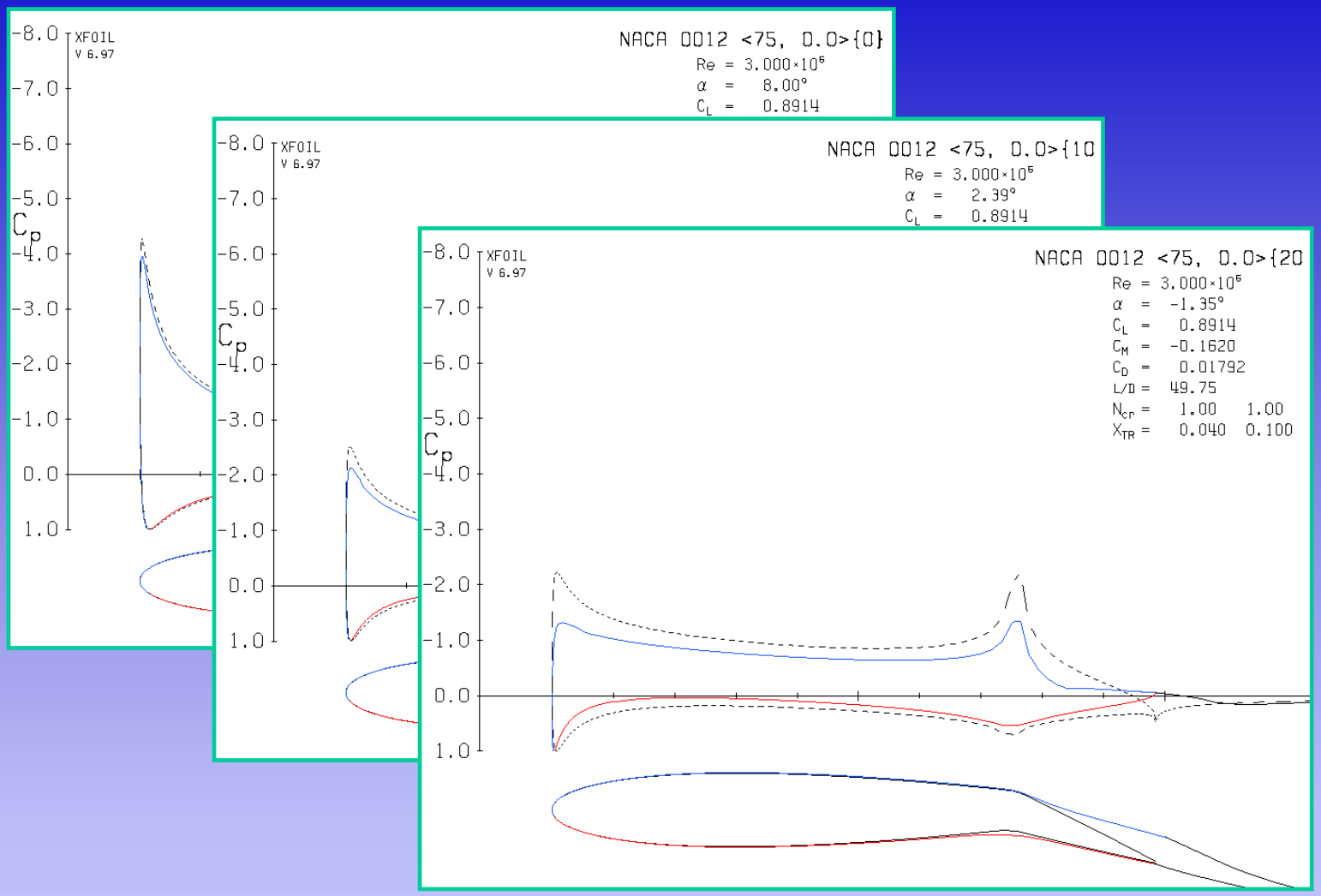

HIGHT LIFT DEVICES

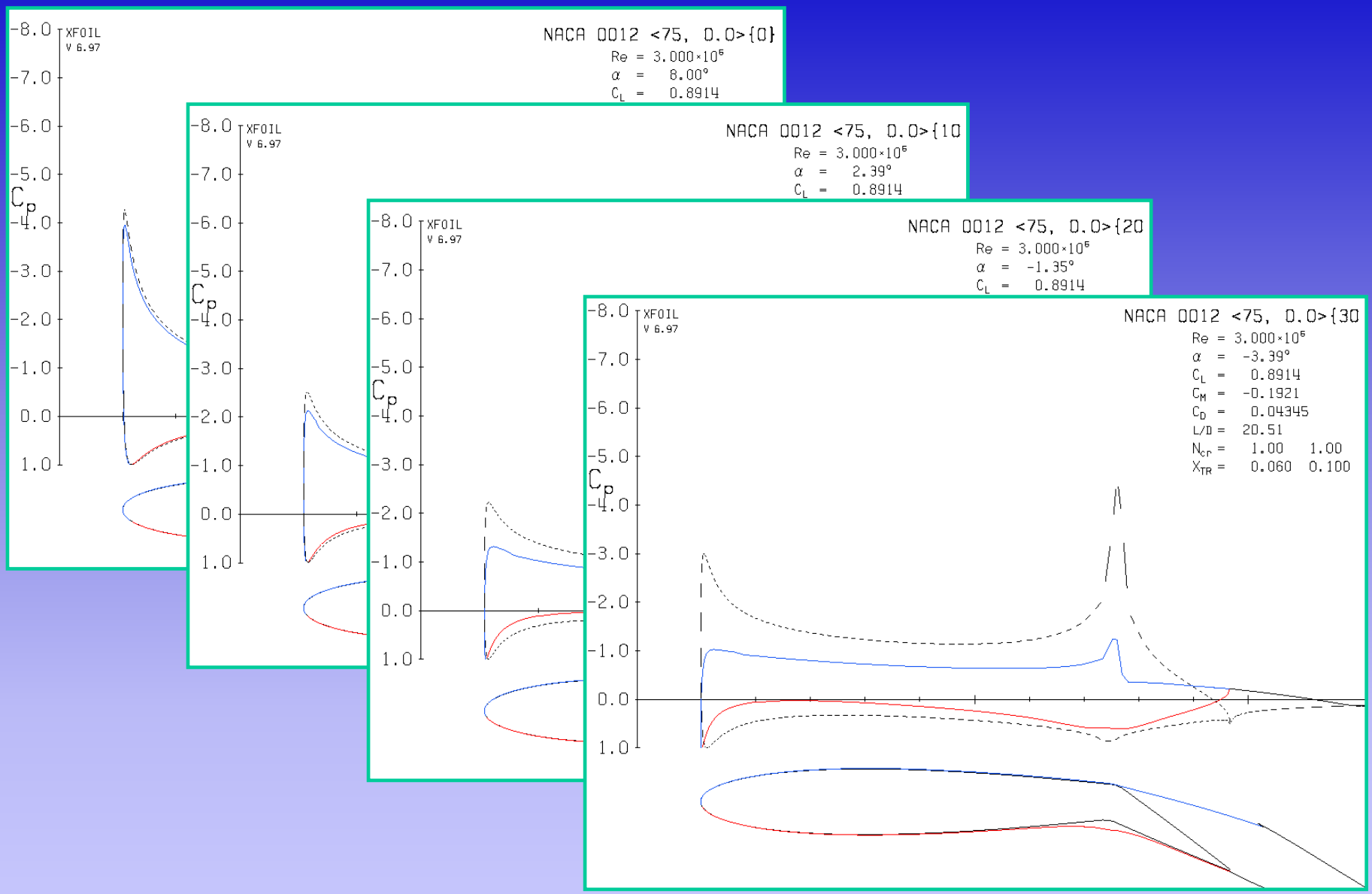

HIGHT LIFT DEVICES

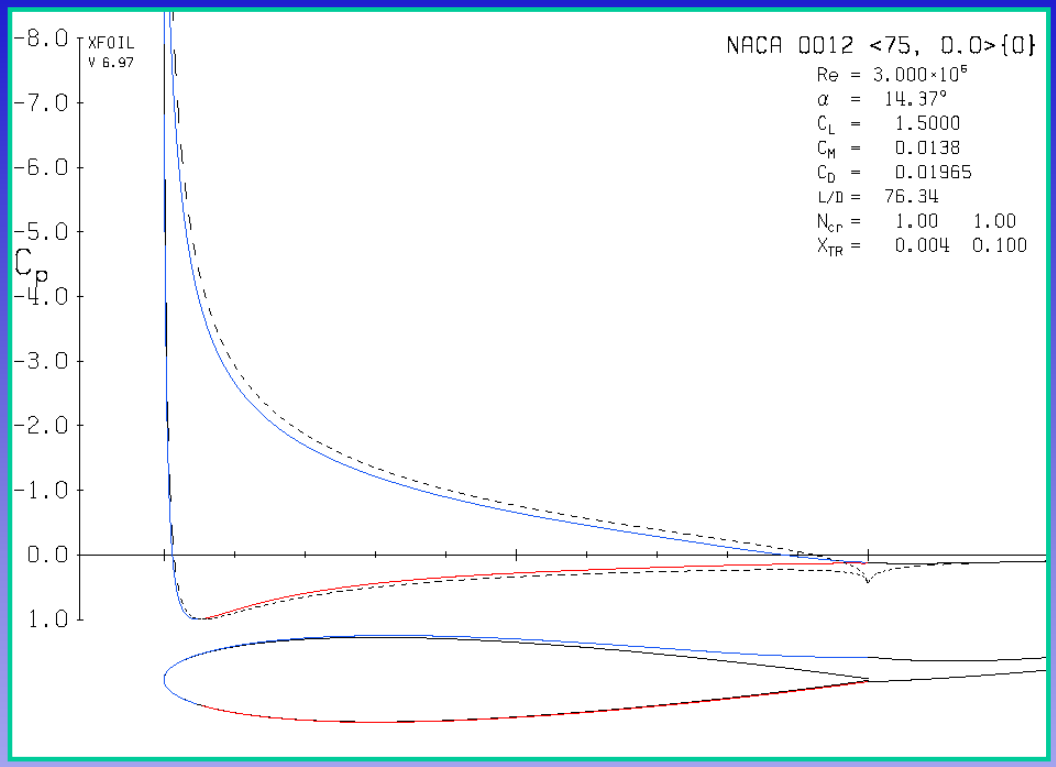

HIGHT LIFT DEVICES

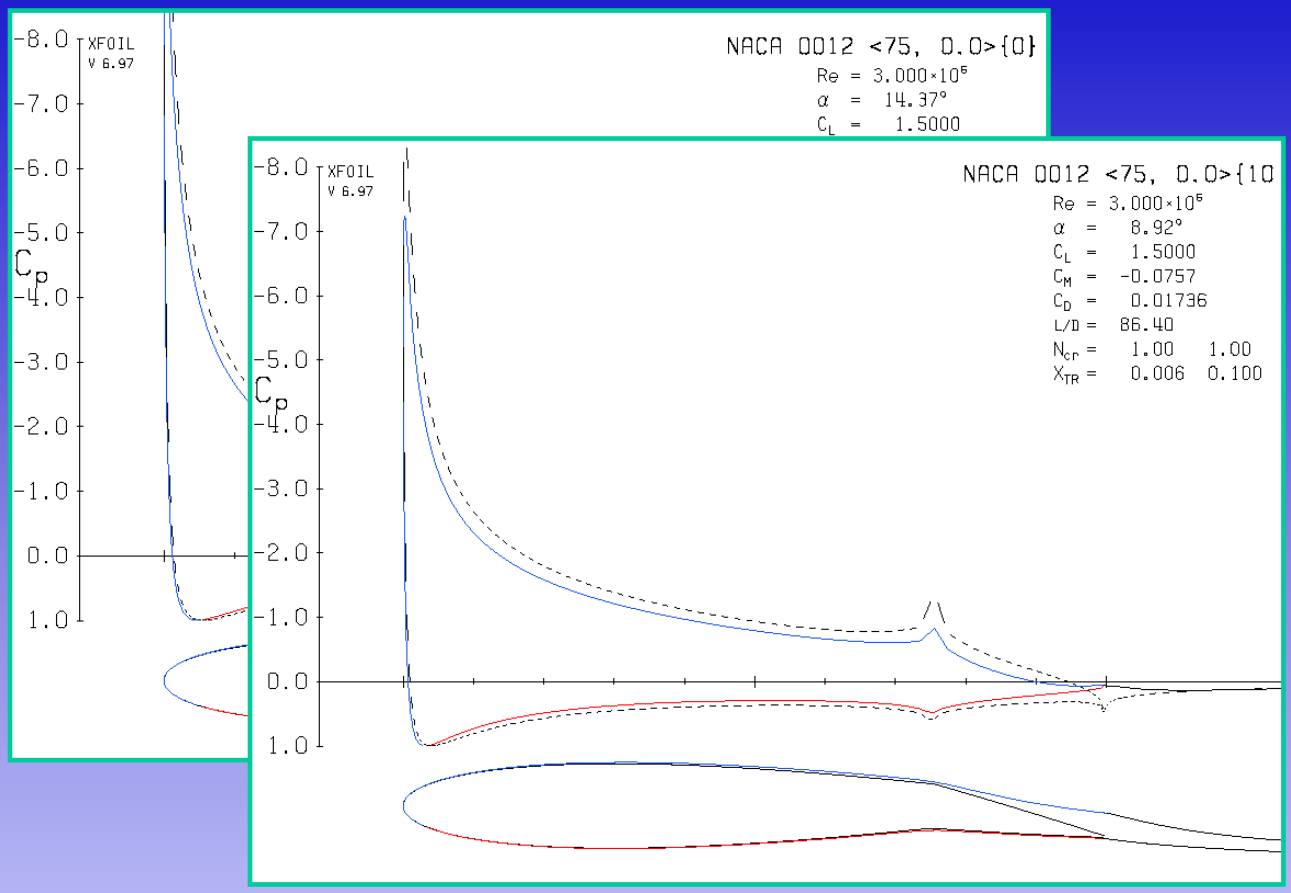

HIGHT LIFT DEVICES

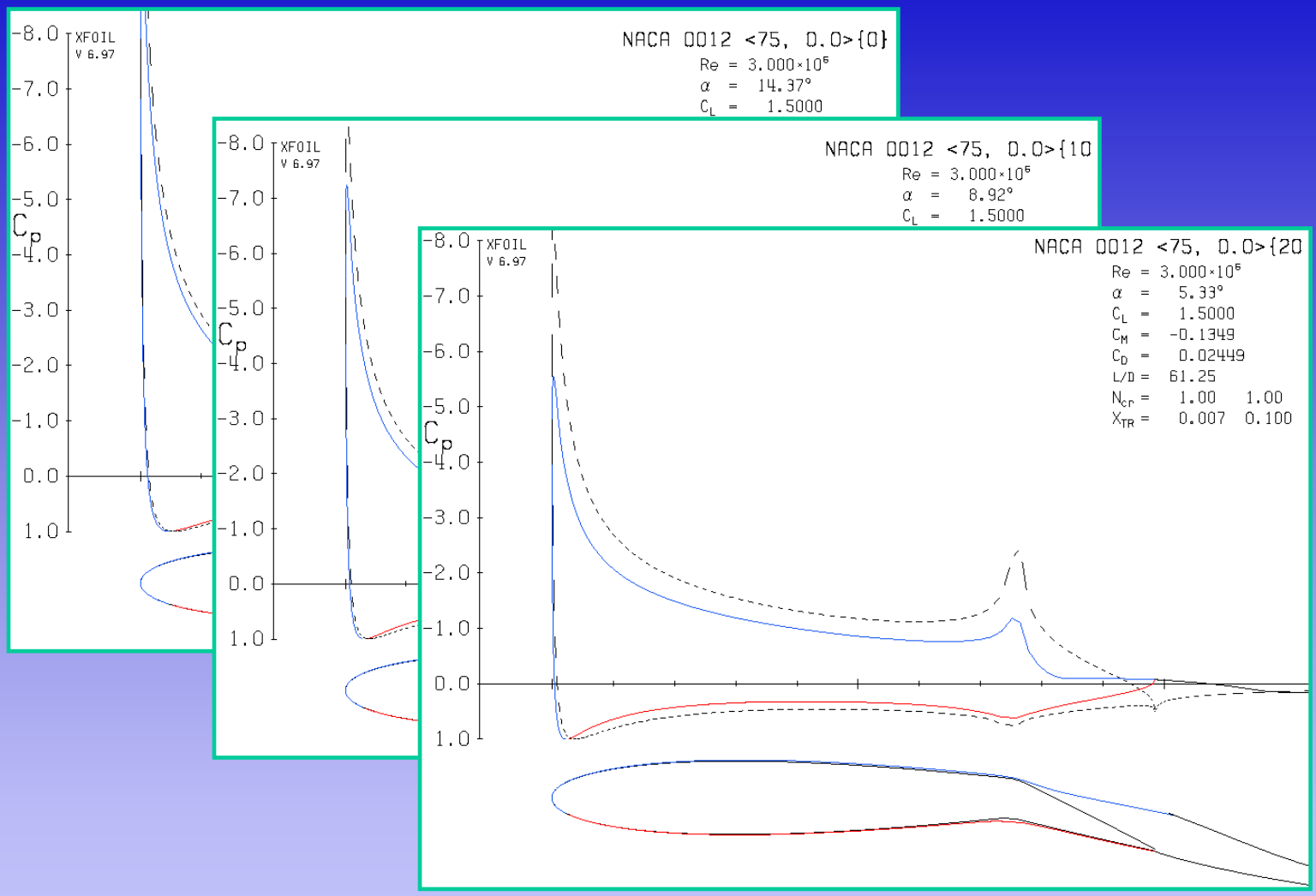

HIGHT LIFT DEVICES

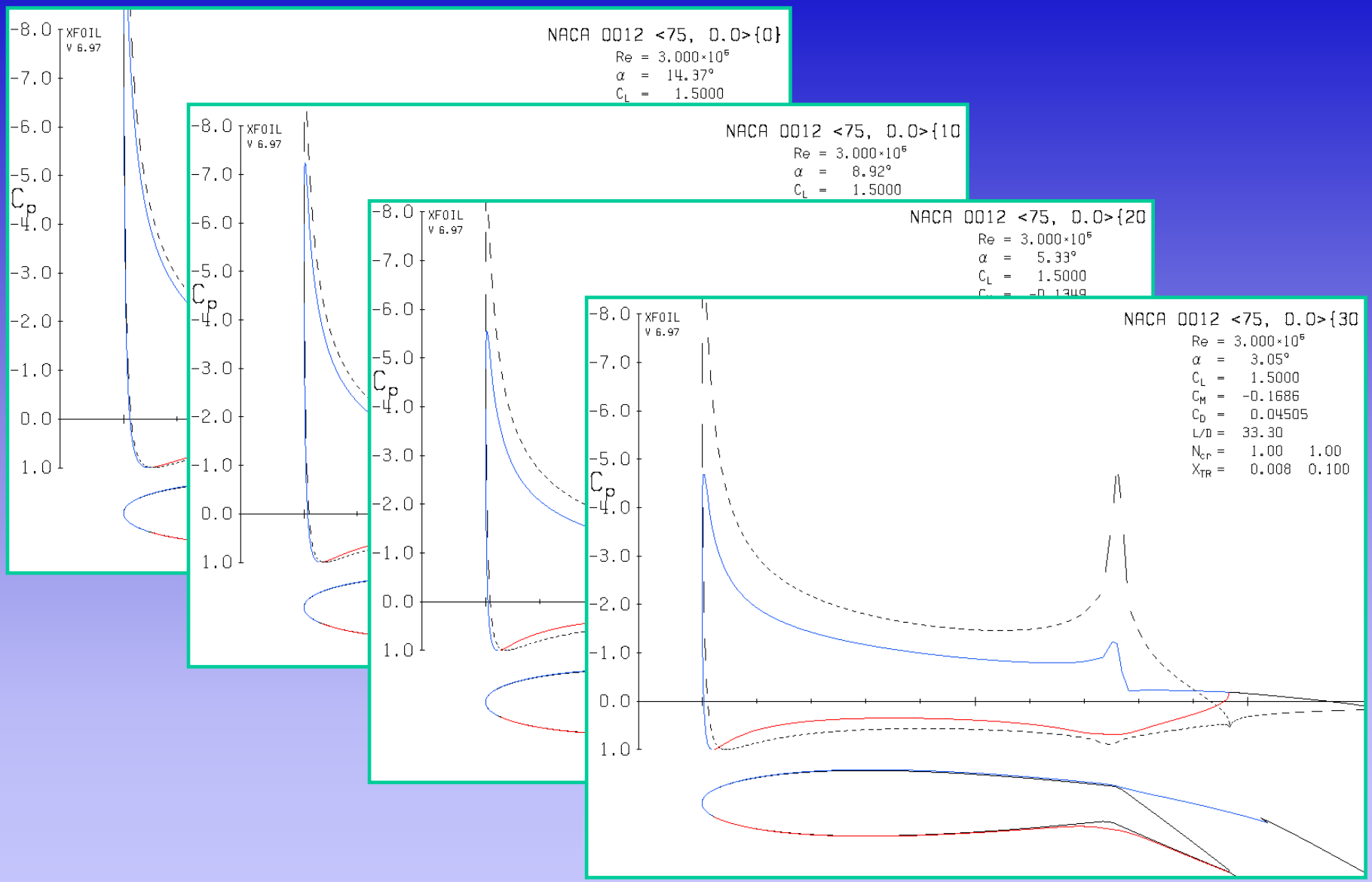

HIGHT LIFT DEVICES

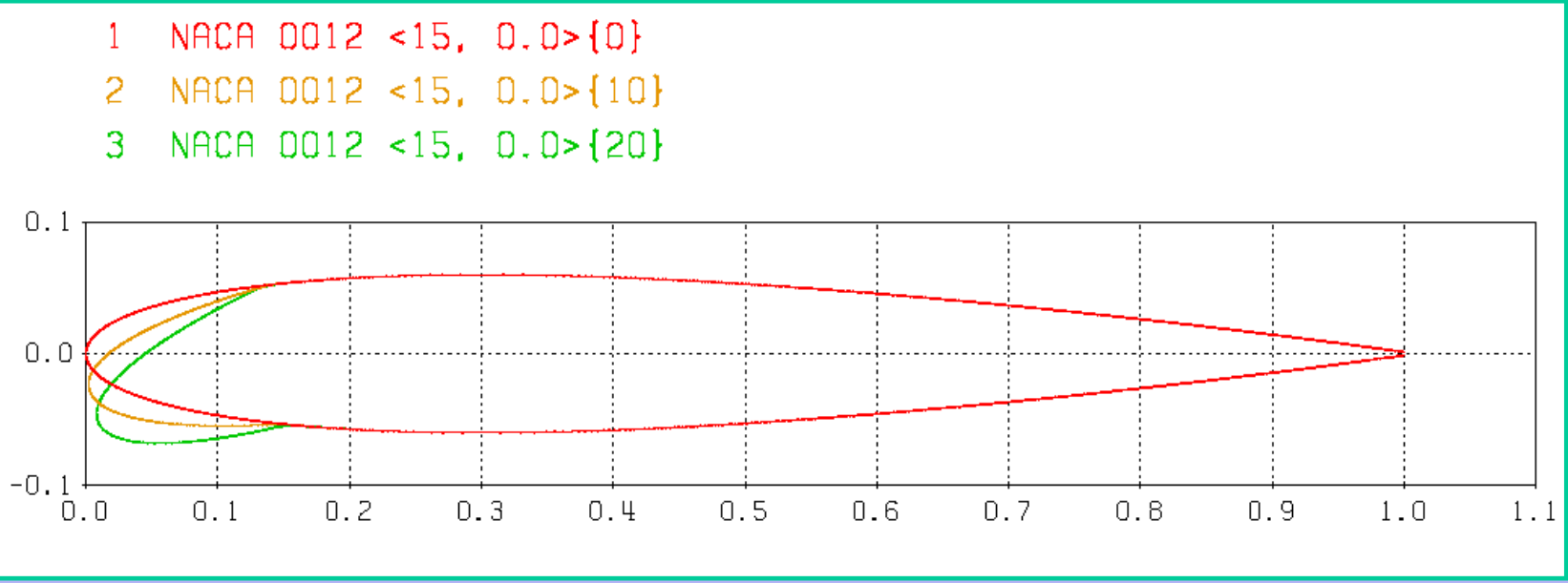

HIGHT LIFT DEVICES

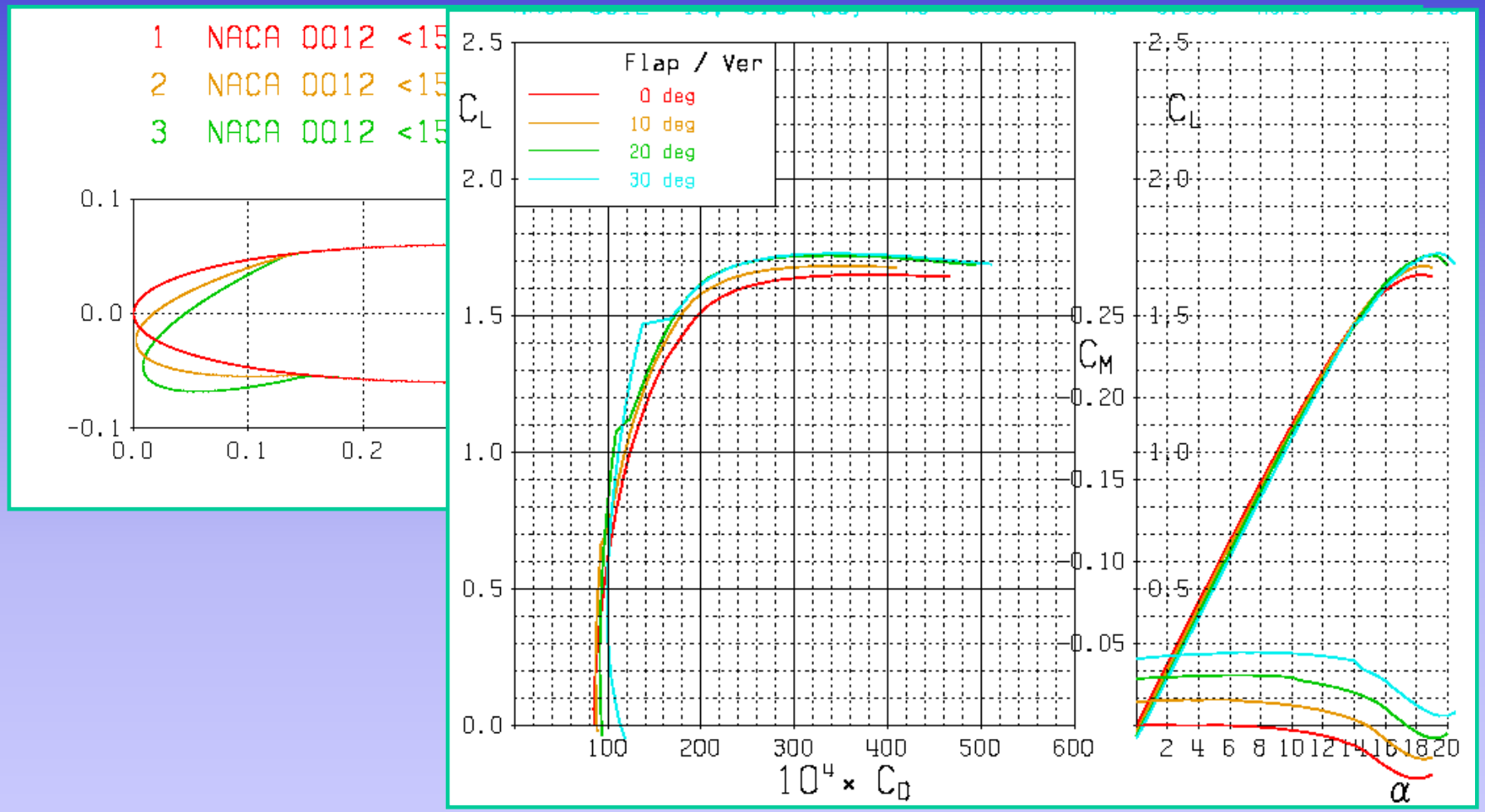

HIGHT LIFT DEVICES

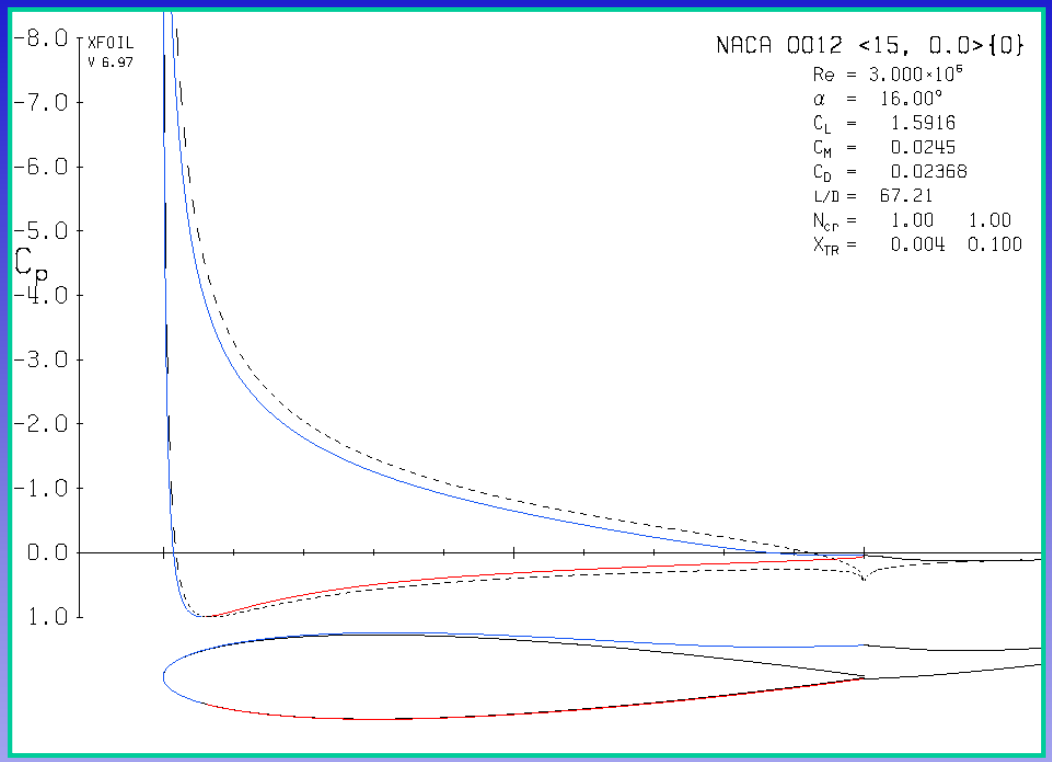

HIGHT LIFT DEVICES

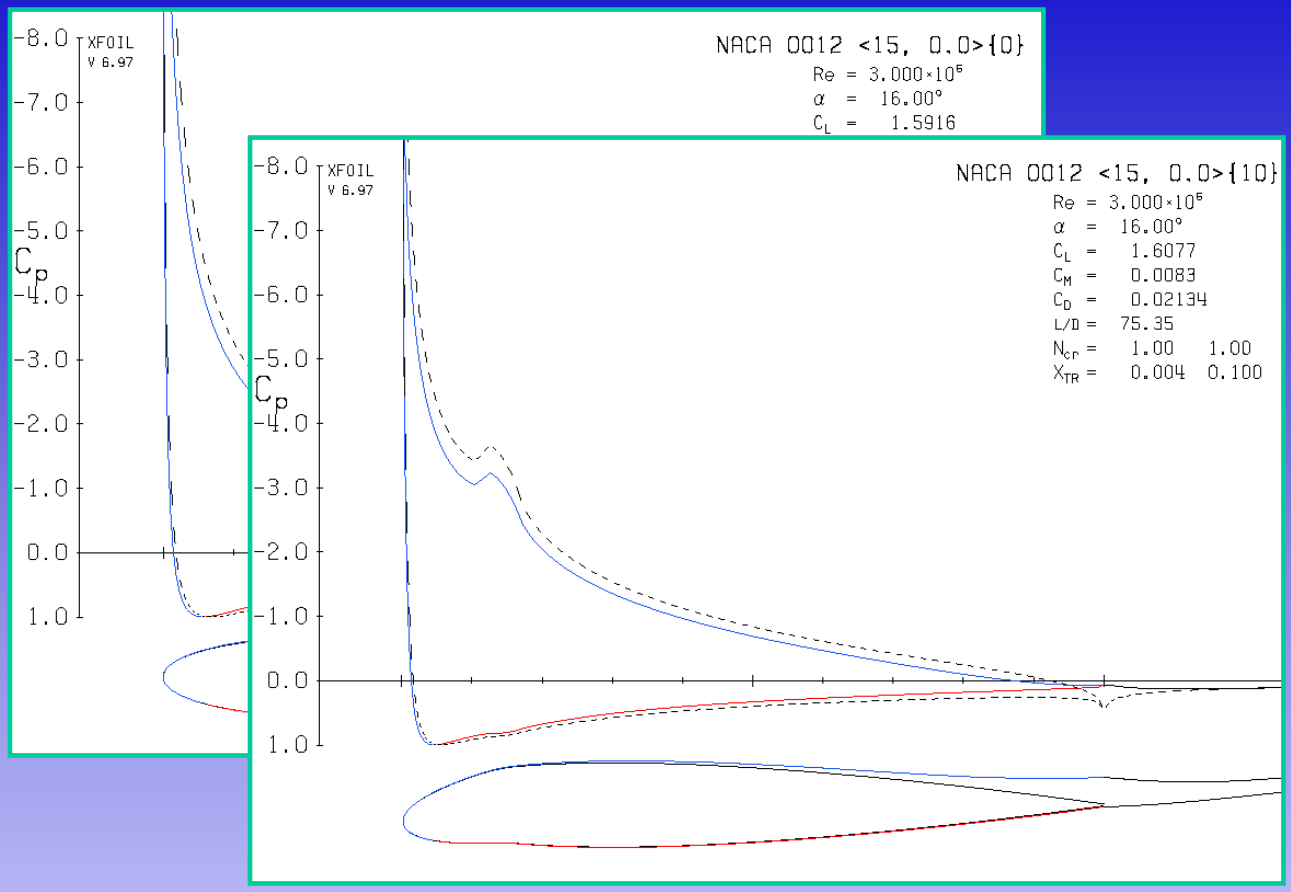

HIGHT LIFT DEVICES

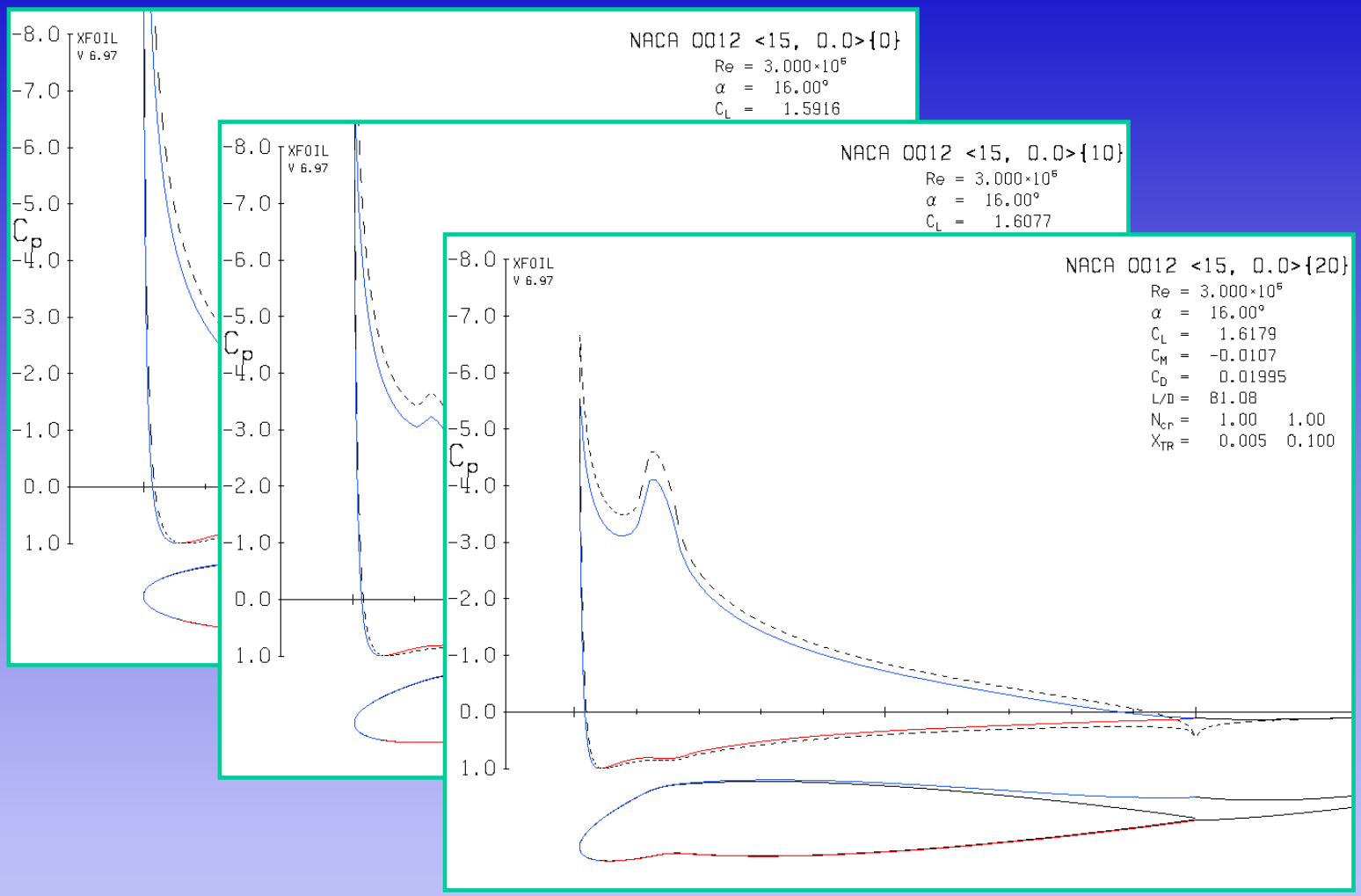

HIGHT LIFT DEVICES

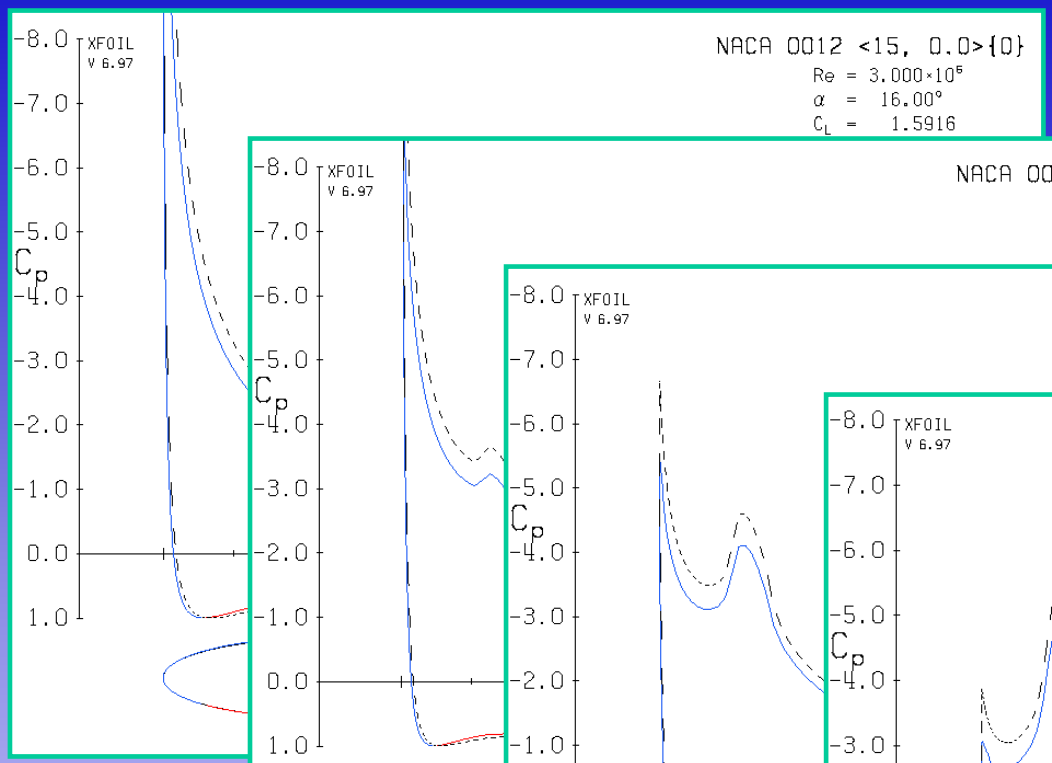

CL_{MAX} V_{MIN} α_{CR}

HIGHT LIFT DEVICES

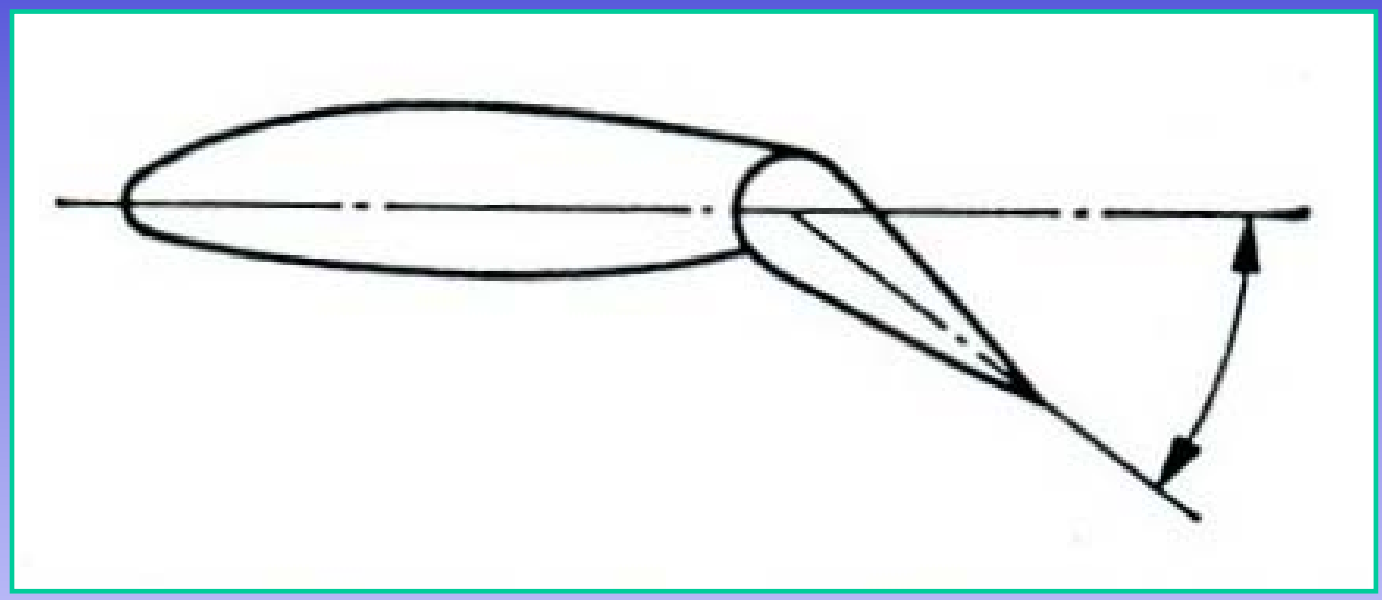

HIGHT LIFT DEVICES

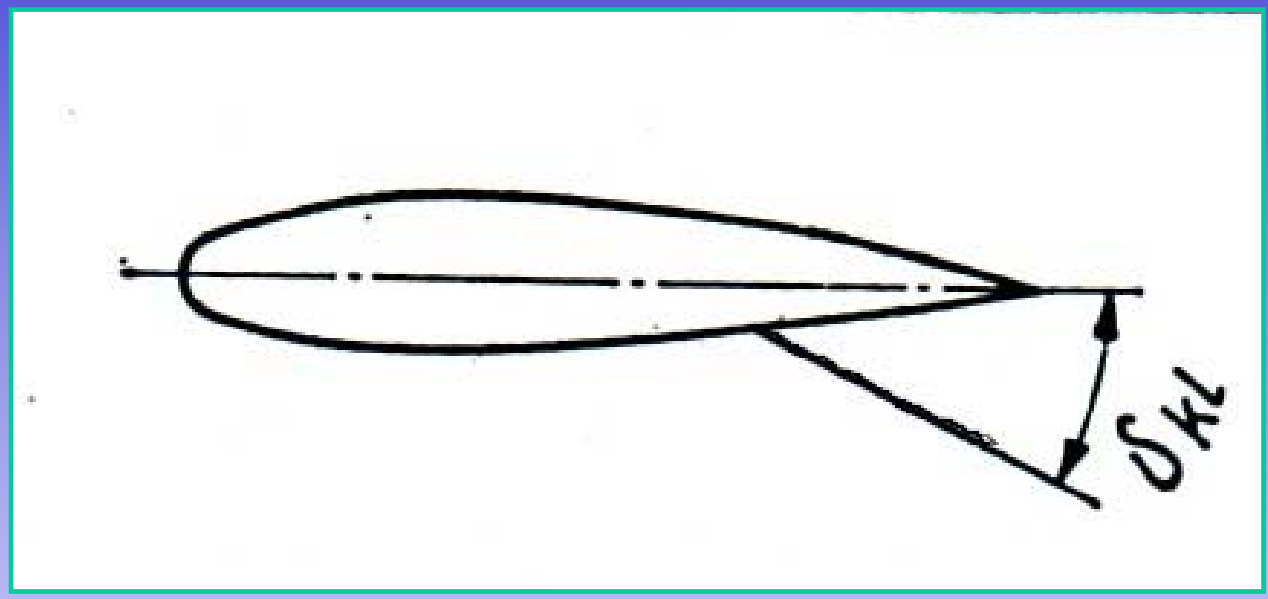

HIGHT LIFT DEVICES

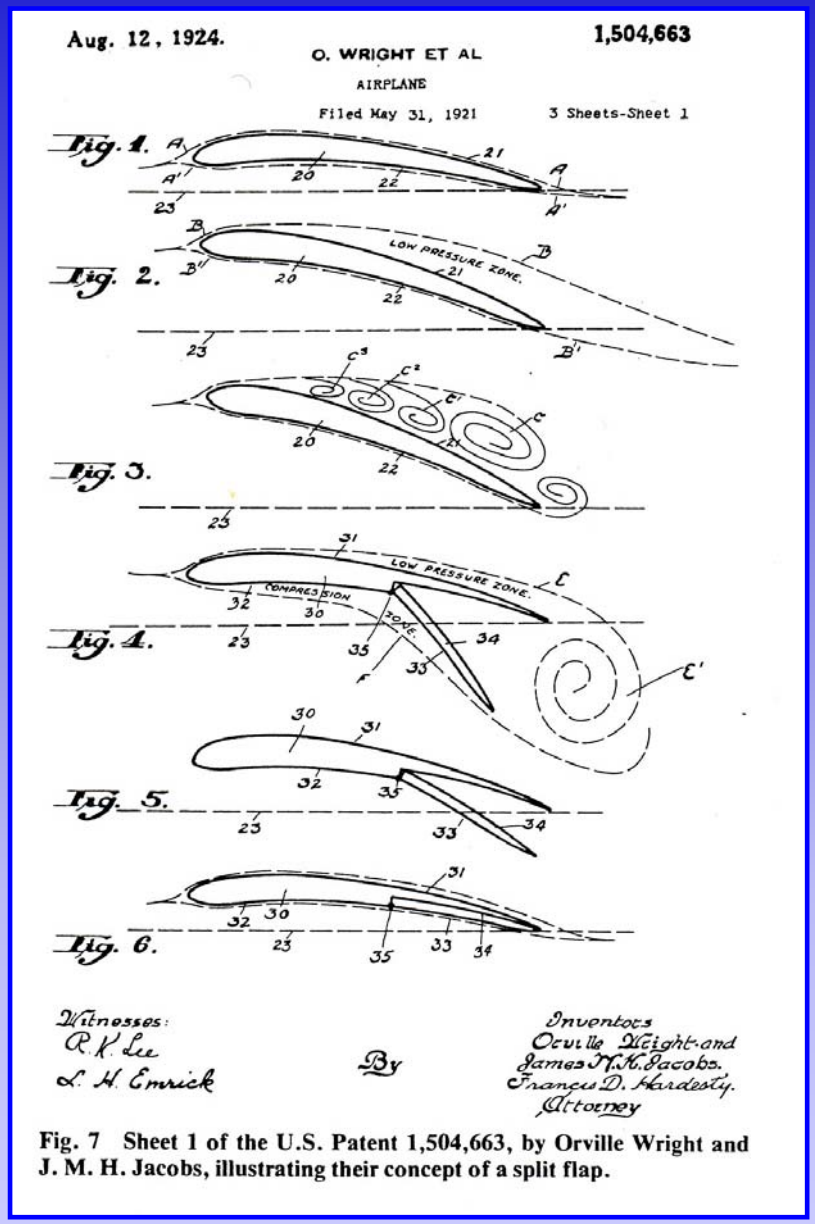

Fig. 7 Sheet 1 of the U.S. Patent 1,504,663, by Orville Wright and J. M. H. Jacobs, illustrating their concept of a split flap.

HIGHT LIFT DEVICES

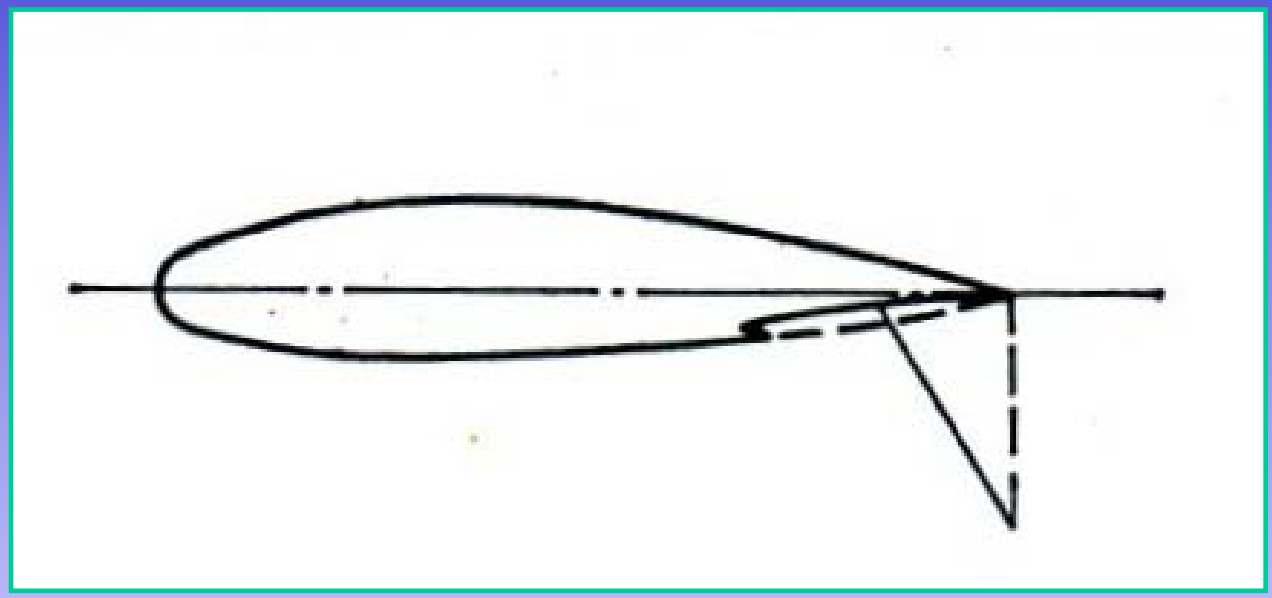

HIGHT LIFT DEVICES

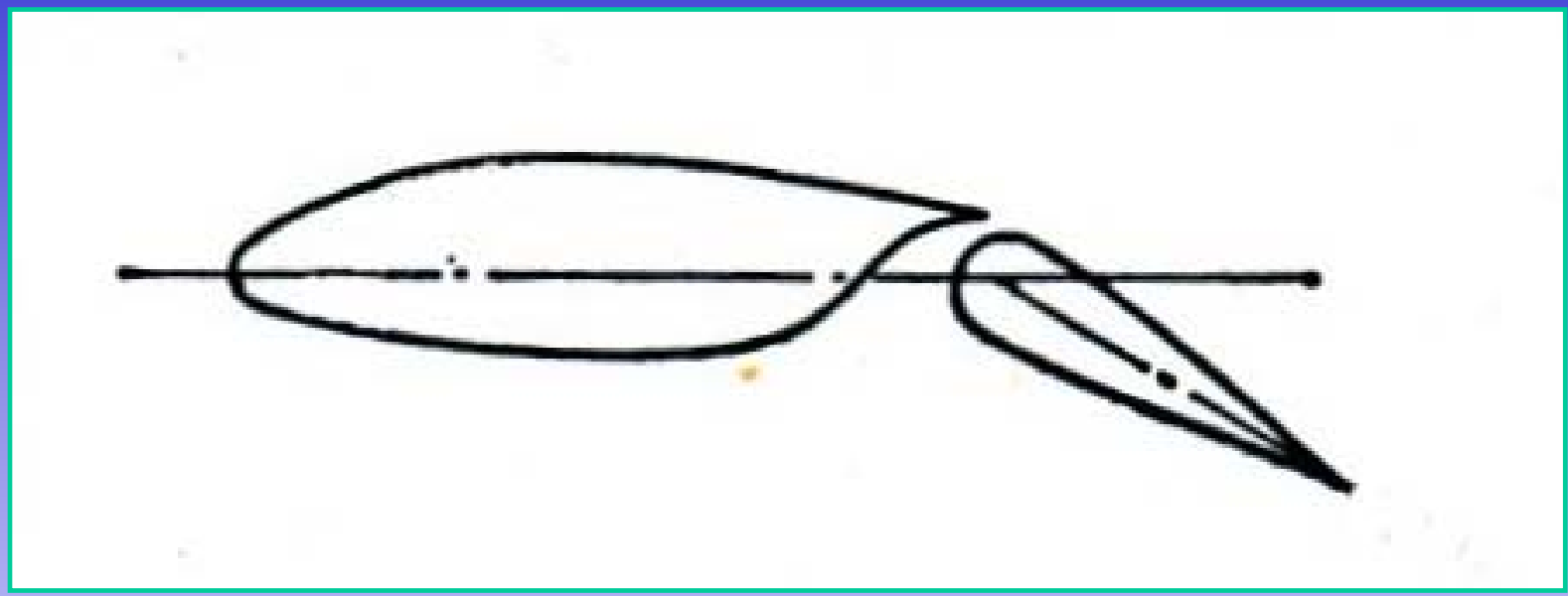

HIGHT LIFT DEVICES

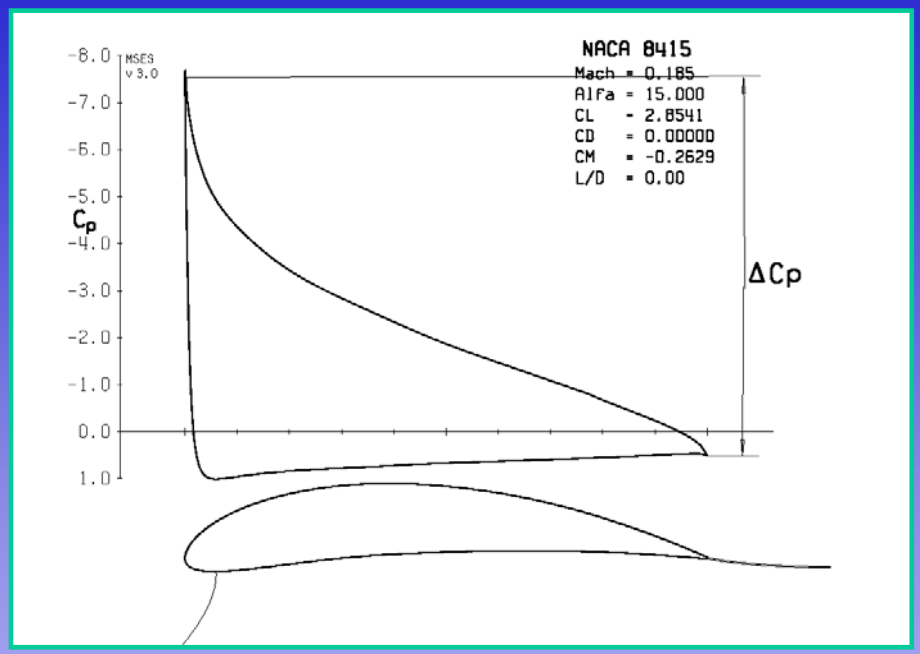

HIGHT LIFT DEVICES

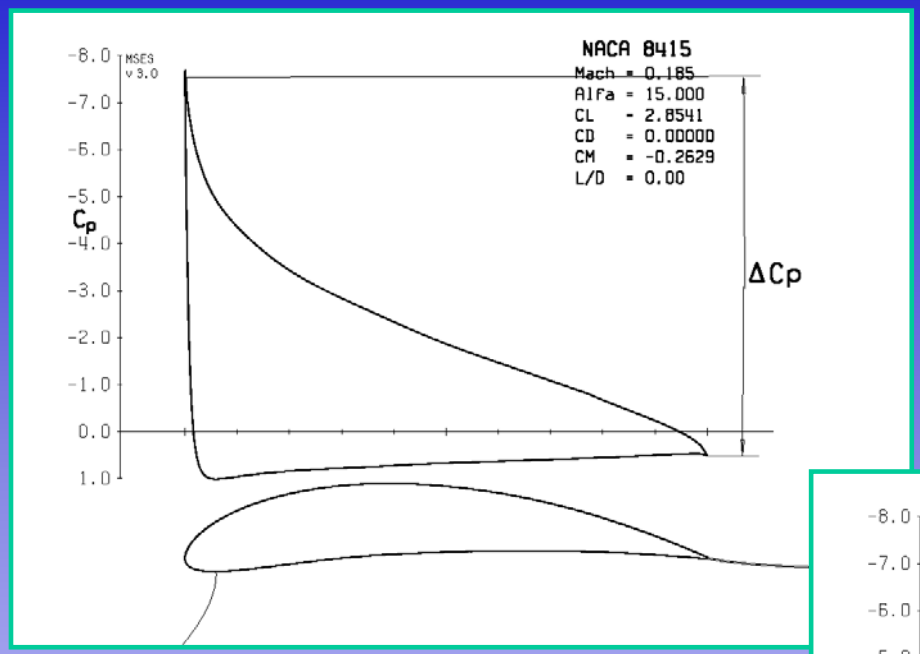

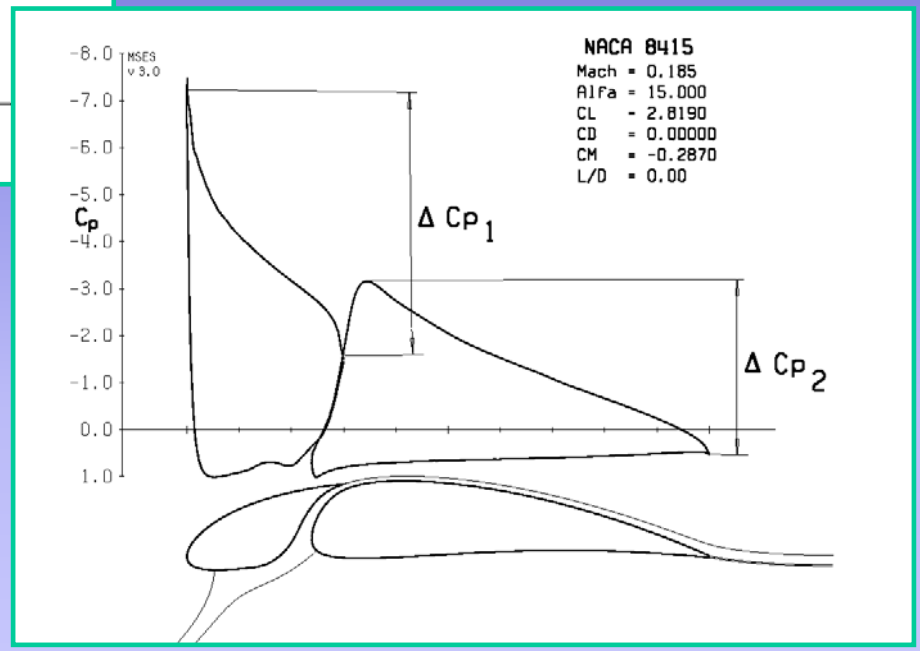

HIGHT LIFT DEVICES

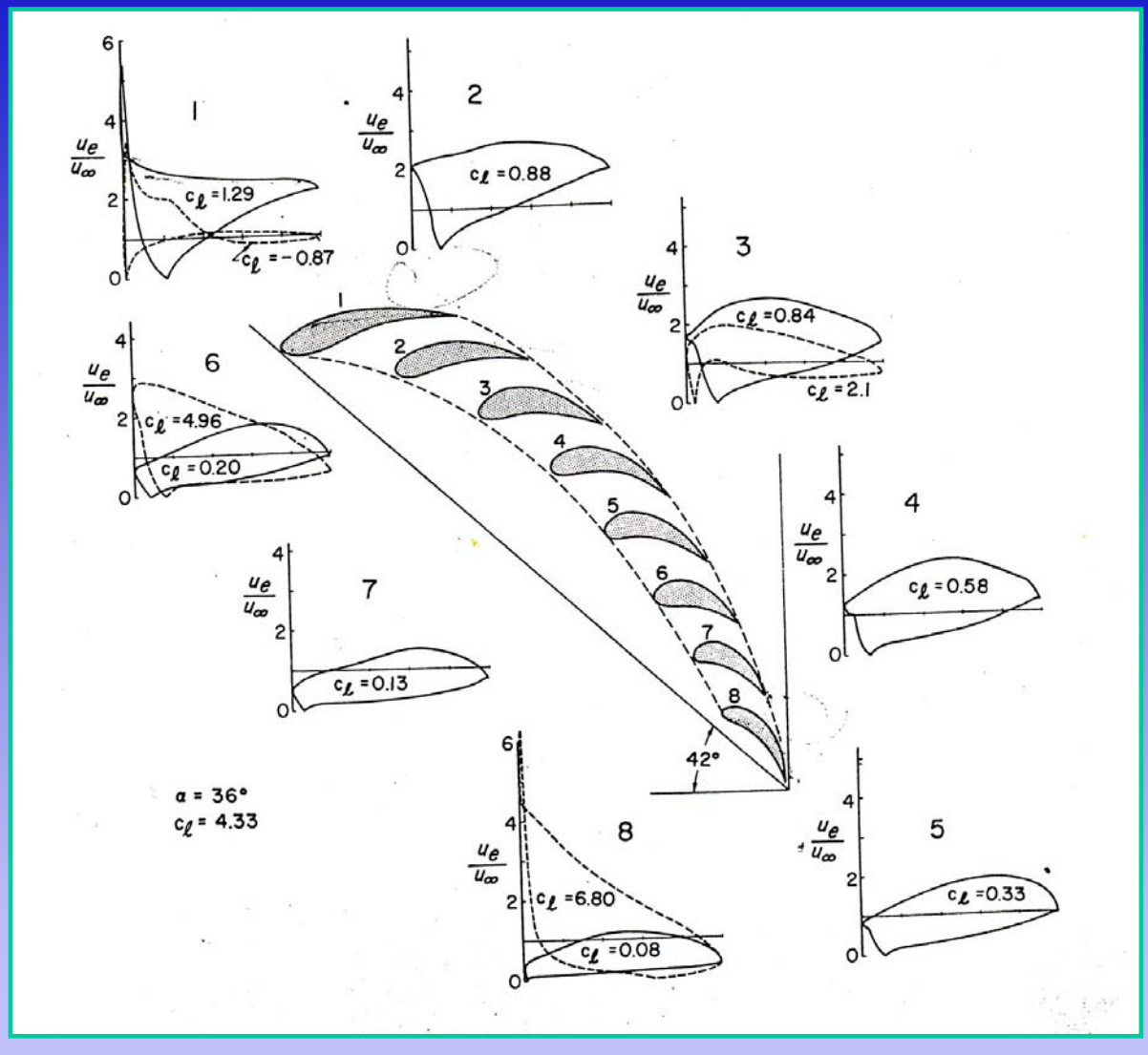

HIGHT LIFT DEVICES

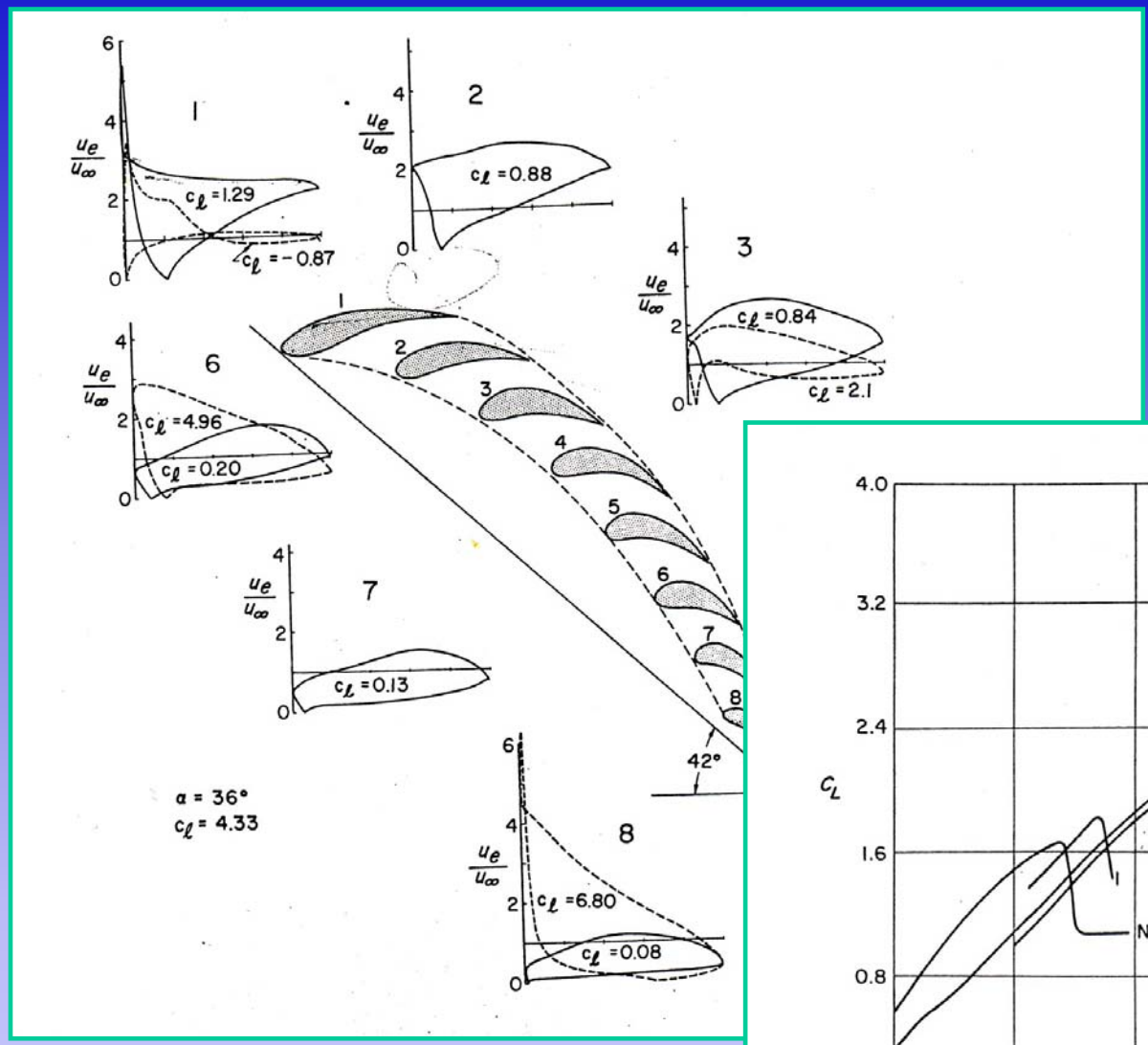

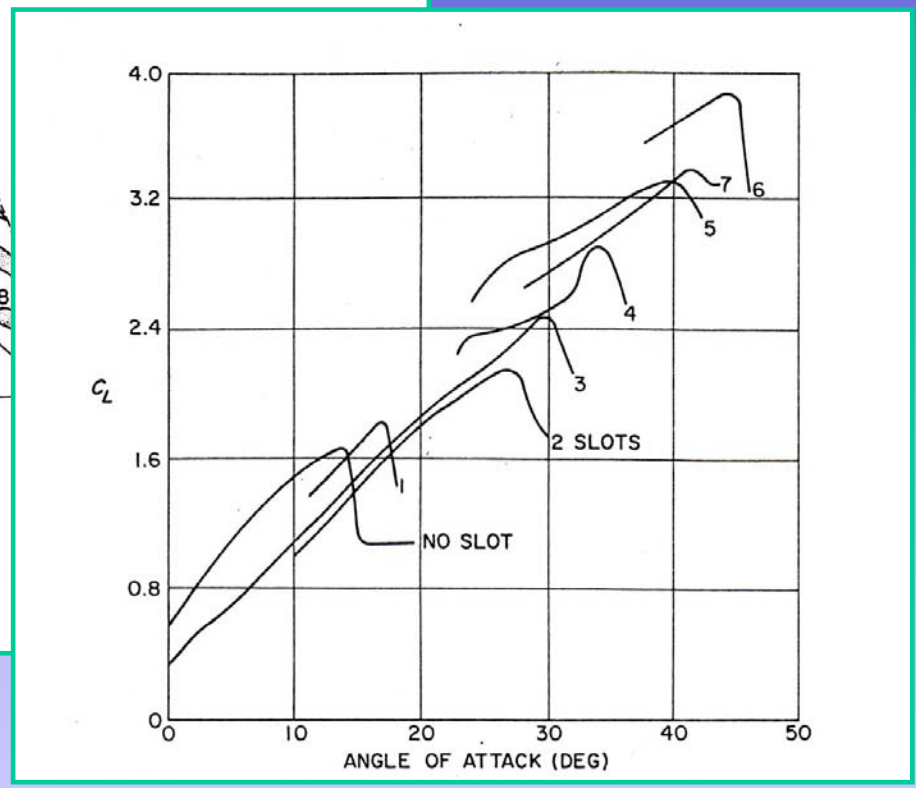

HIGHT LIFT DEVICES

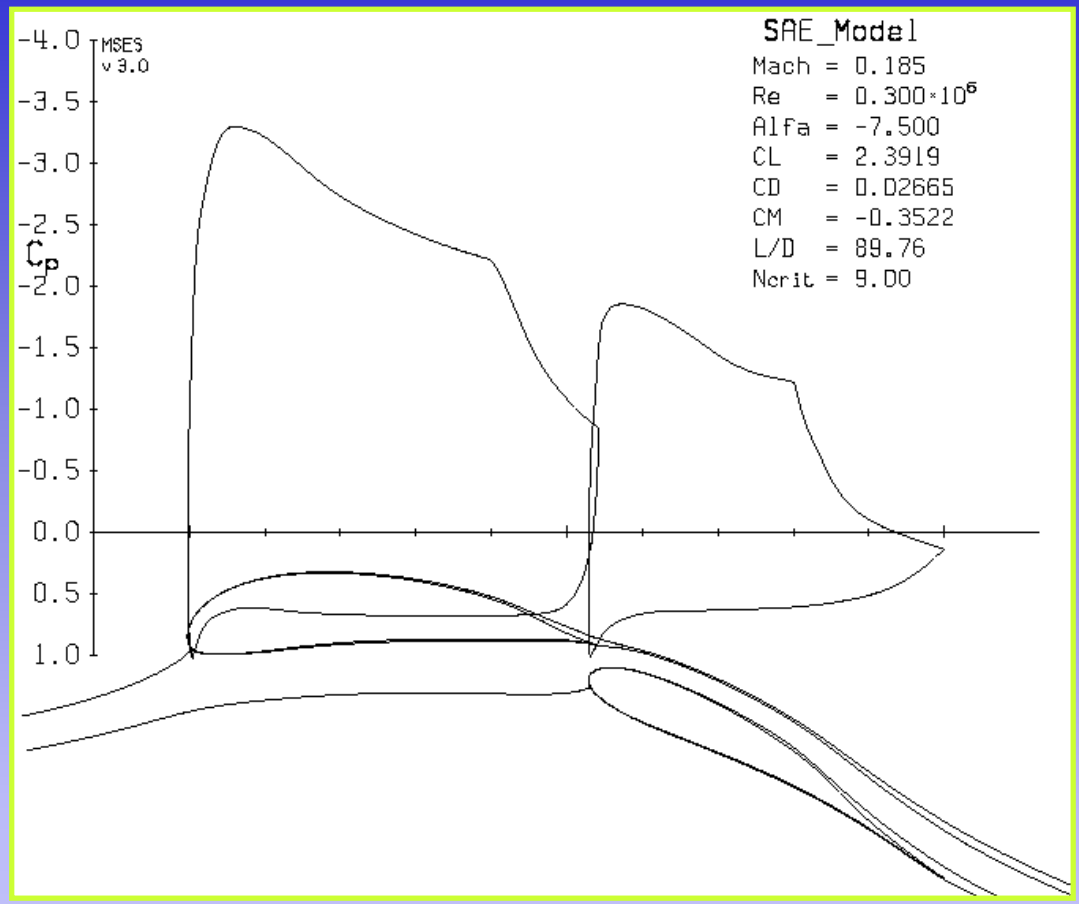

HIGHT LIFT DEVICES

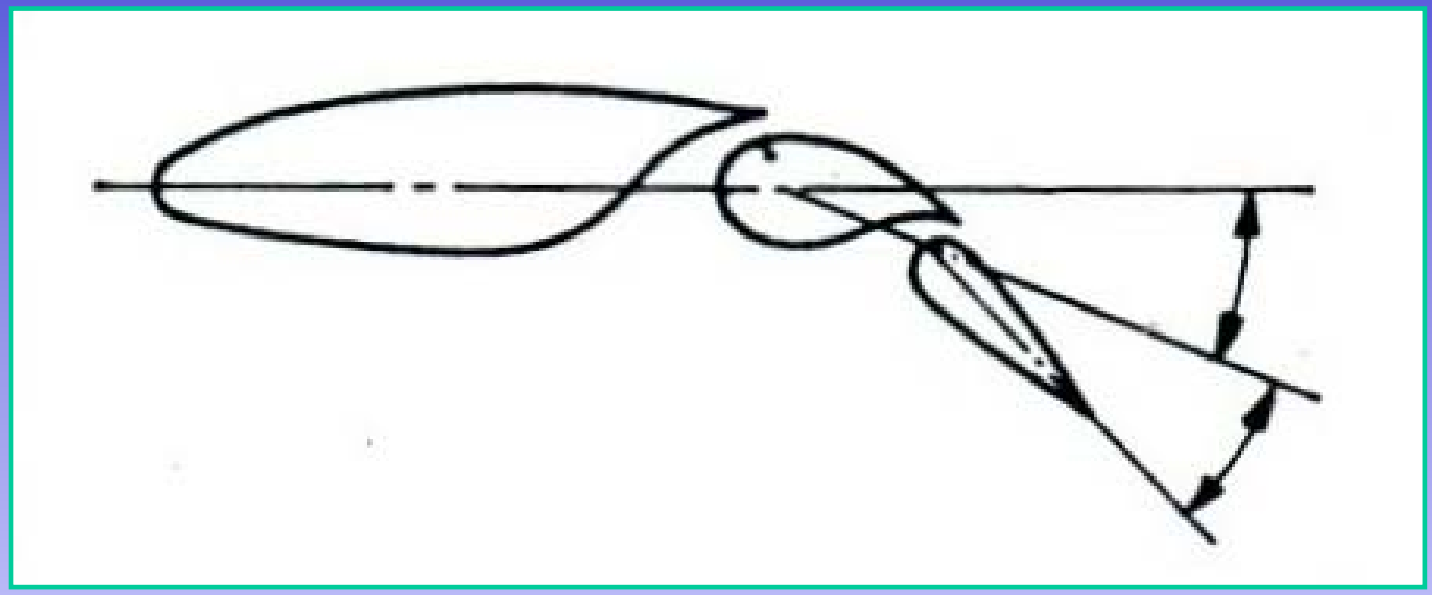

HIGHT LIFT DEVICES

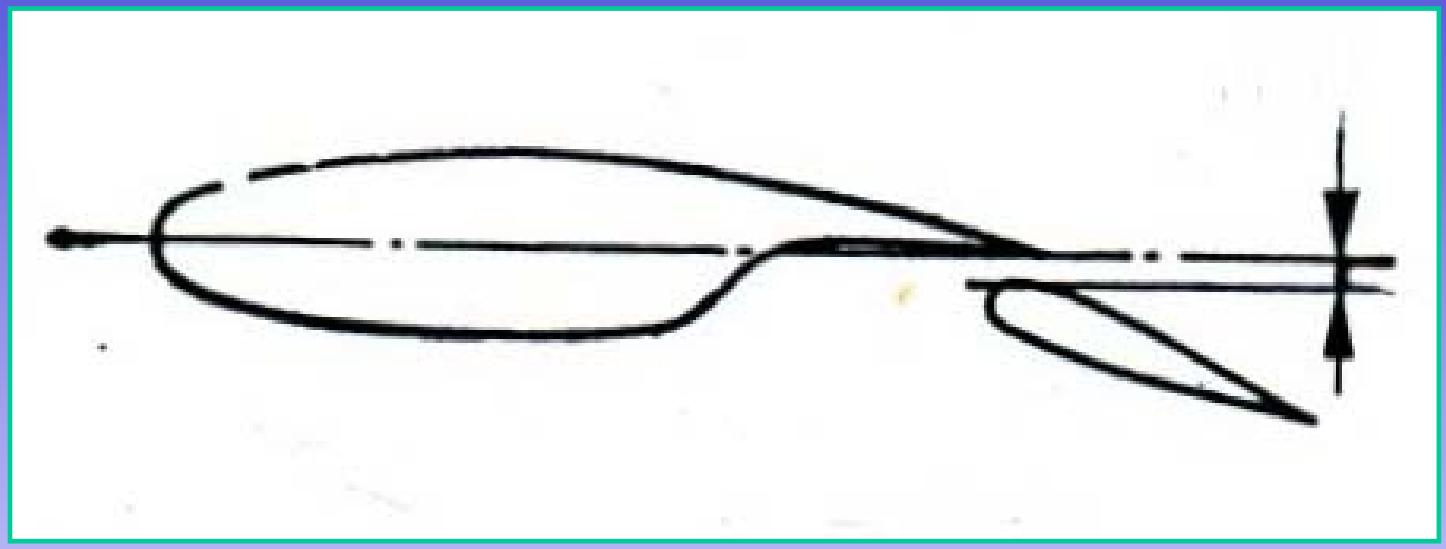

HIGHT LIFT DEVICES

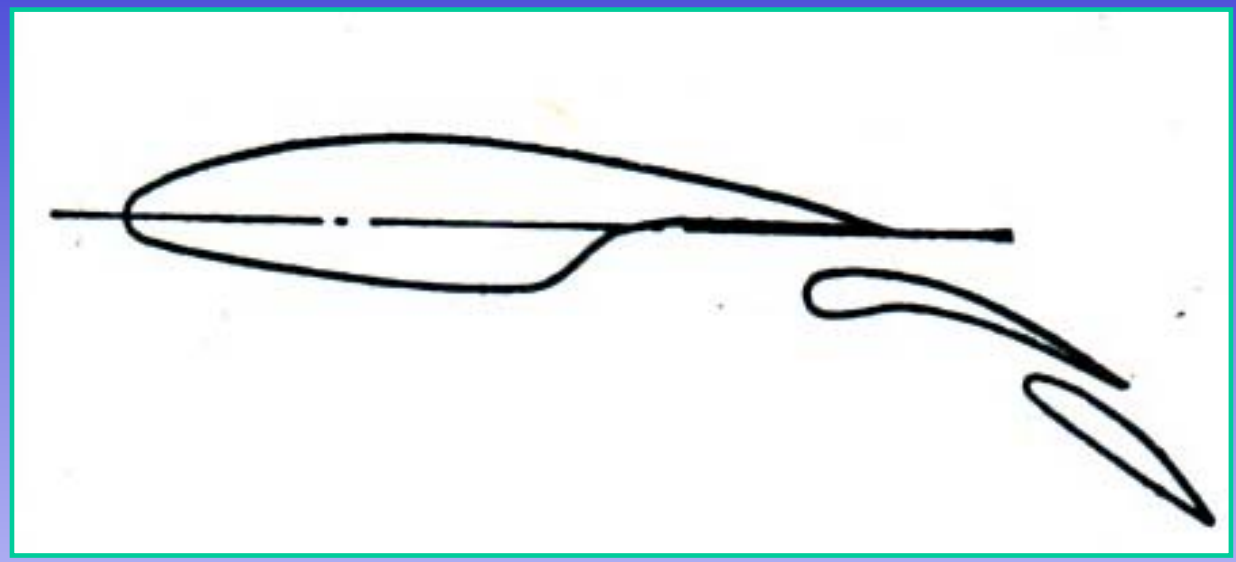

HIGHT LIFT DEVICES

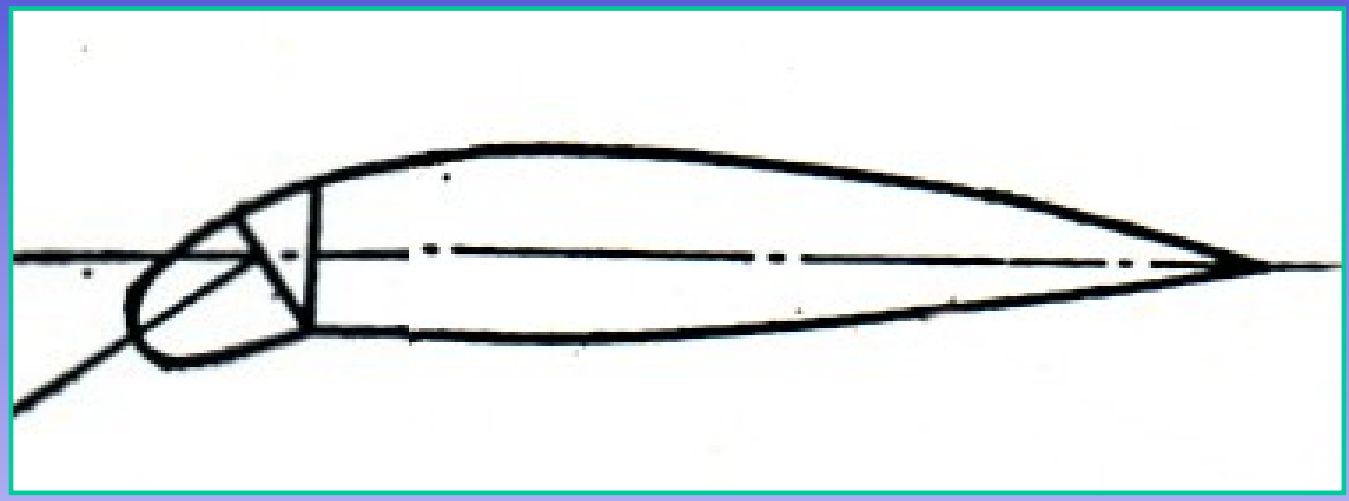

HIGHT LIFT DEVICES

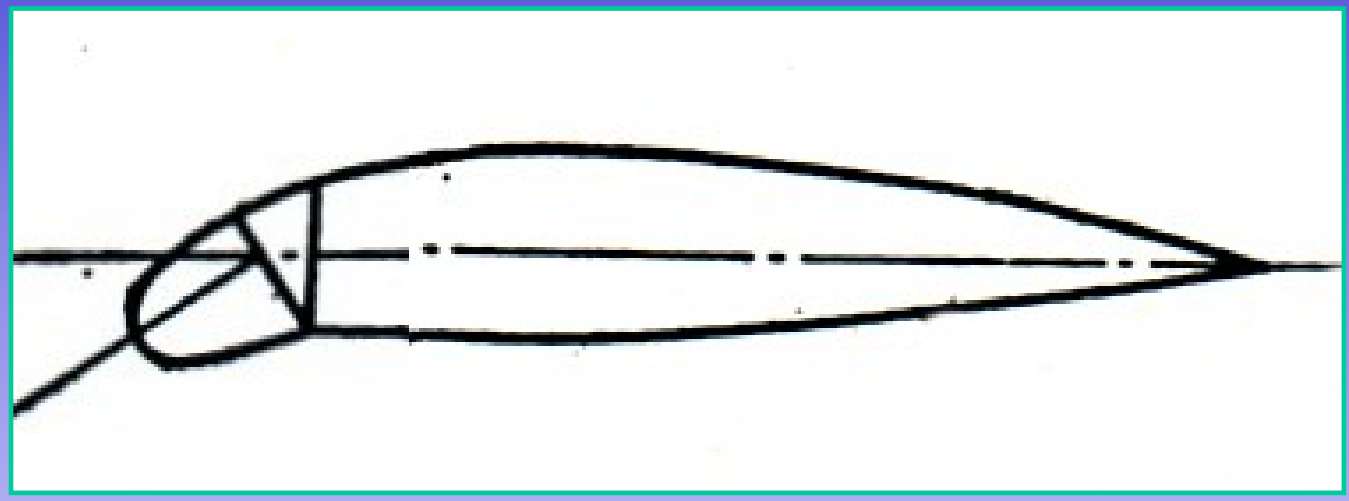

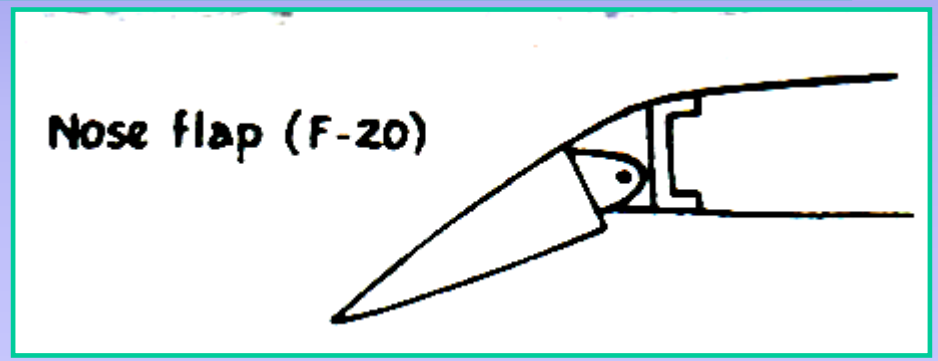

HIGHT LIFT DEVICES

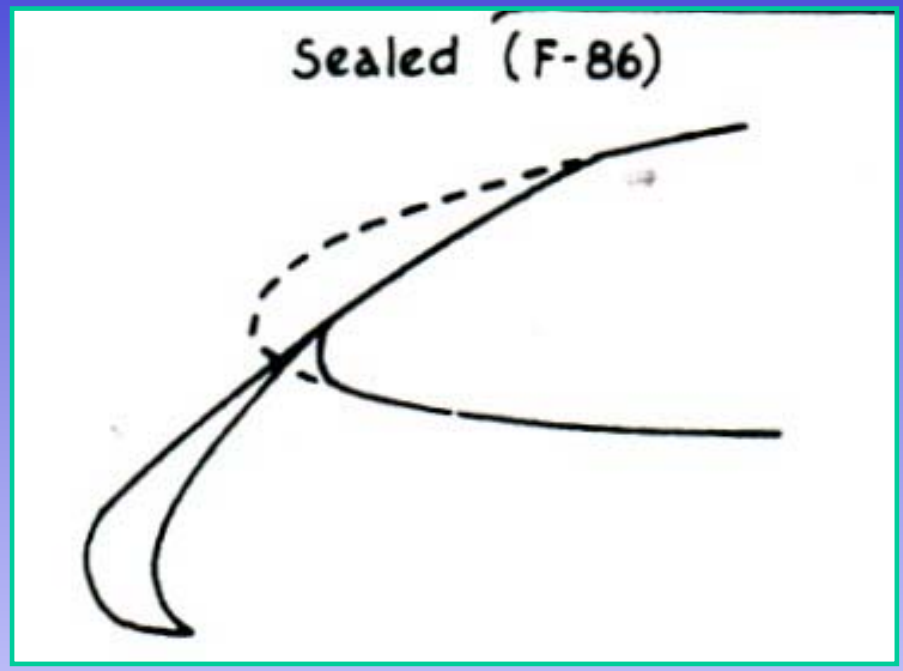

HIGHT LIFT DEVICES

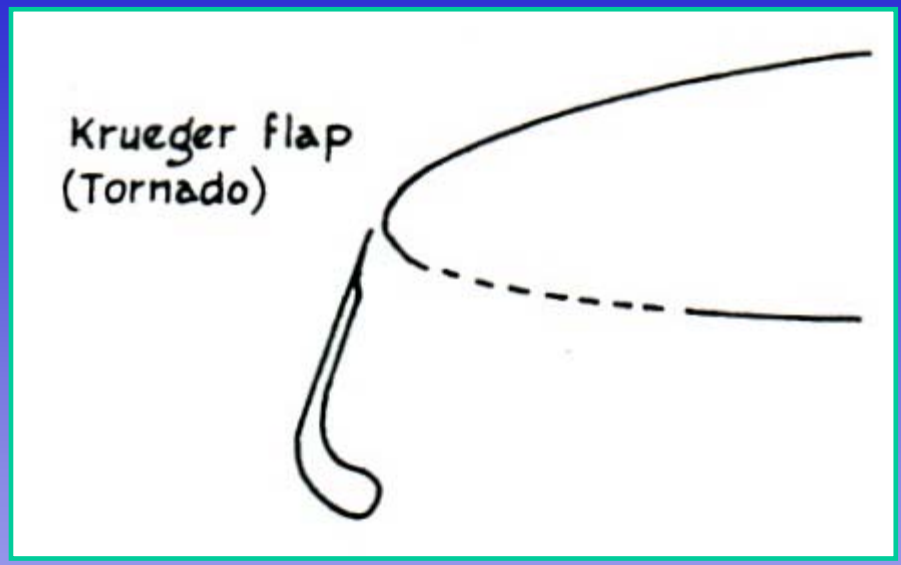

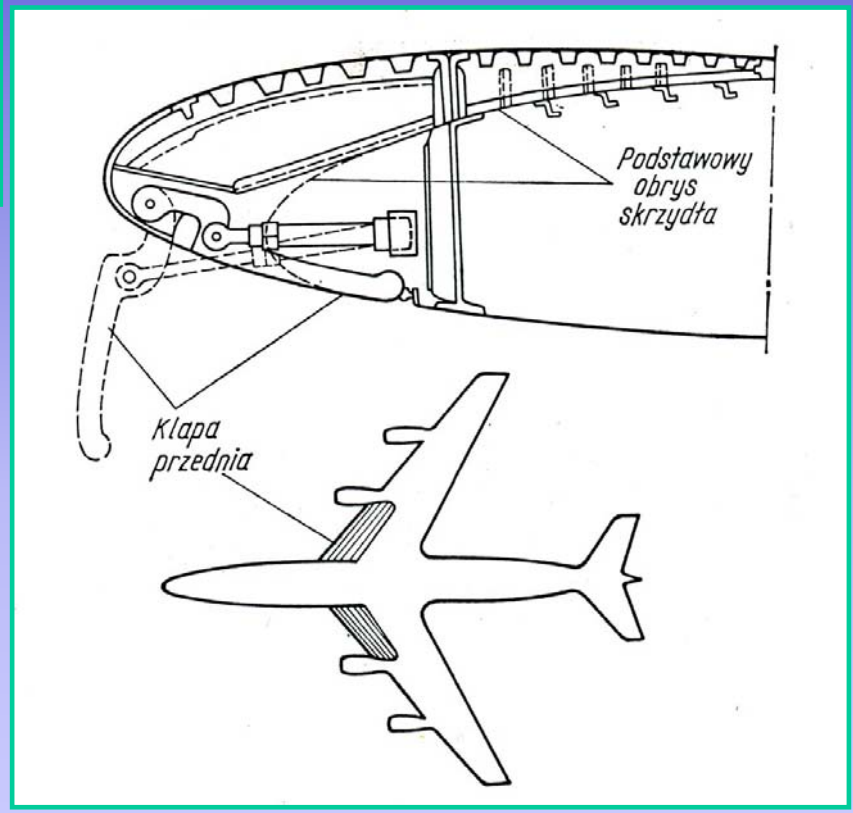

HIGHT LIFT DEVICES

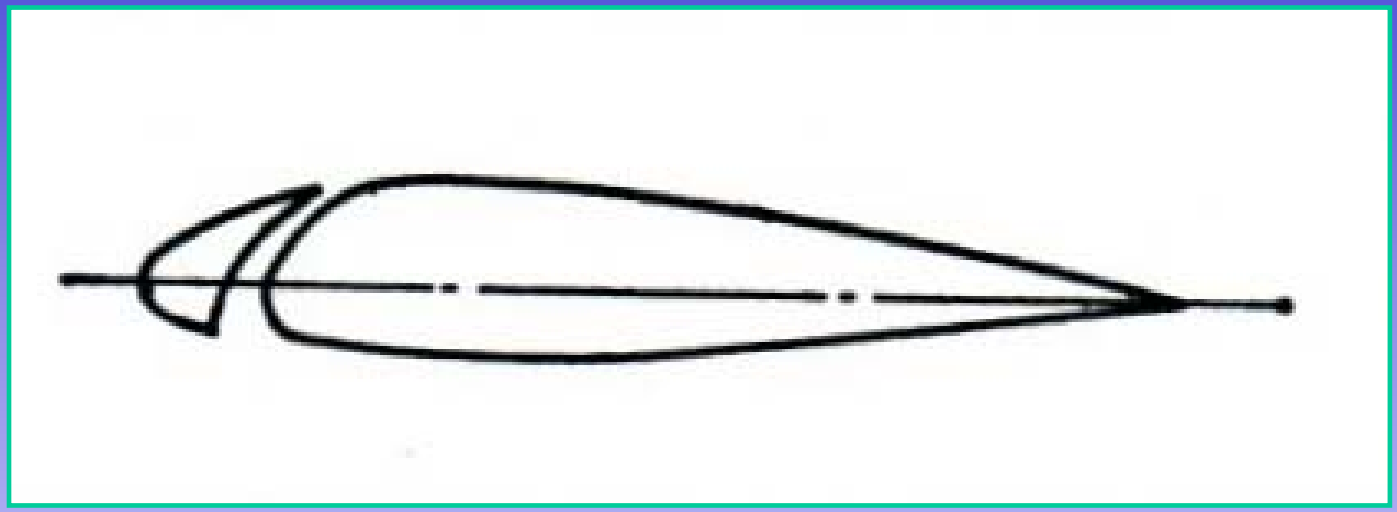

HIGHT LIFT DEVICES

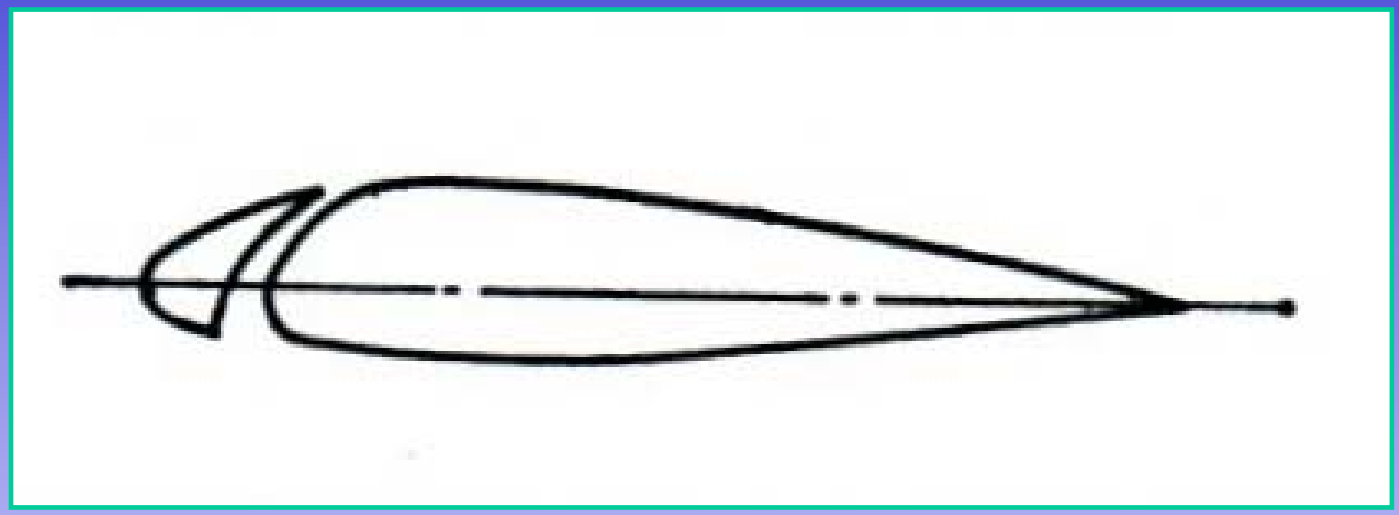

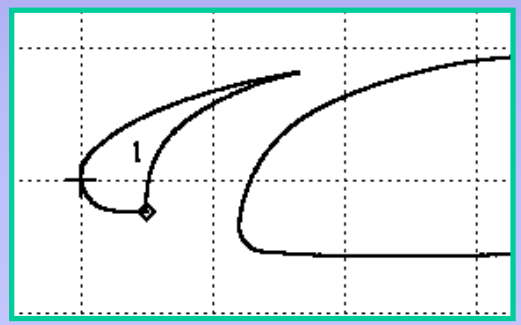

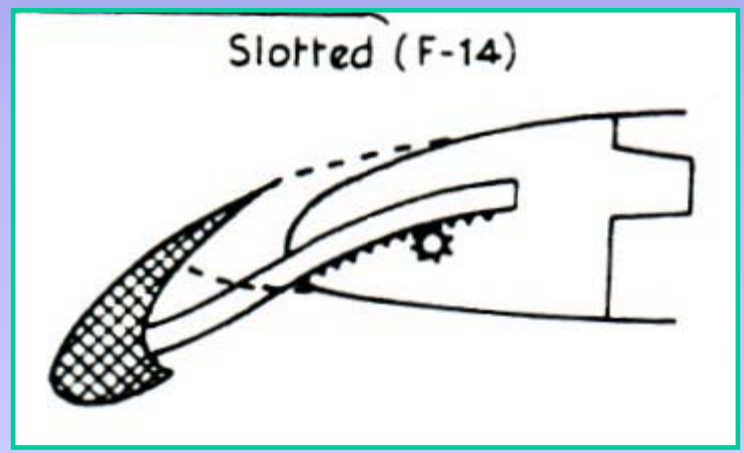

HIGHT LIFT DEVICES

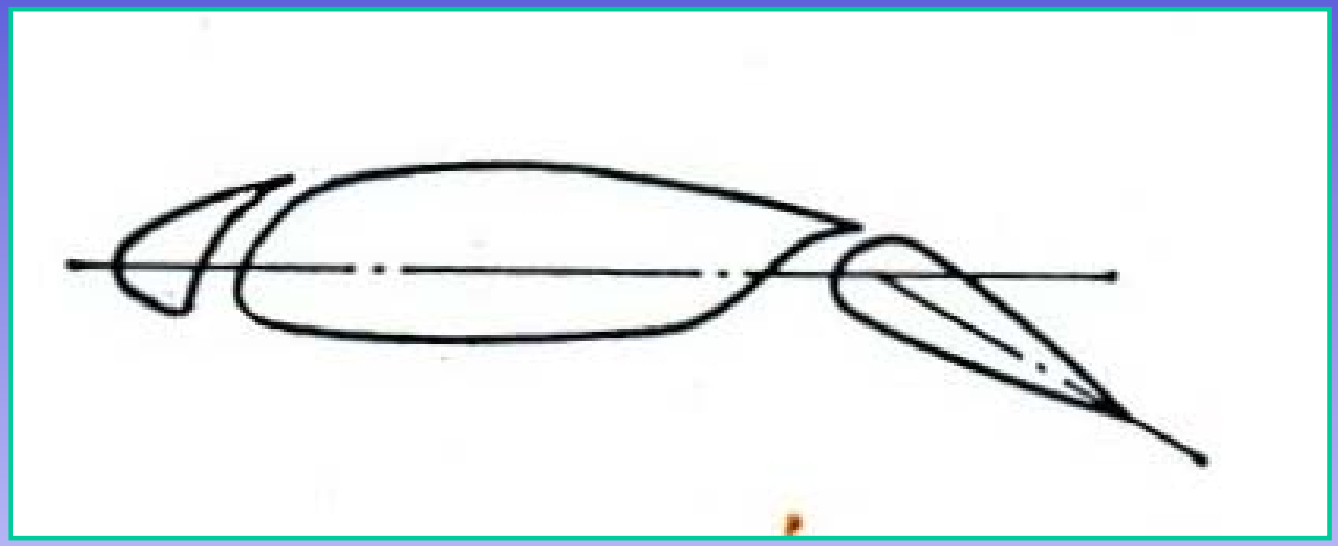

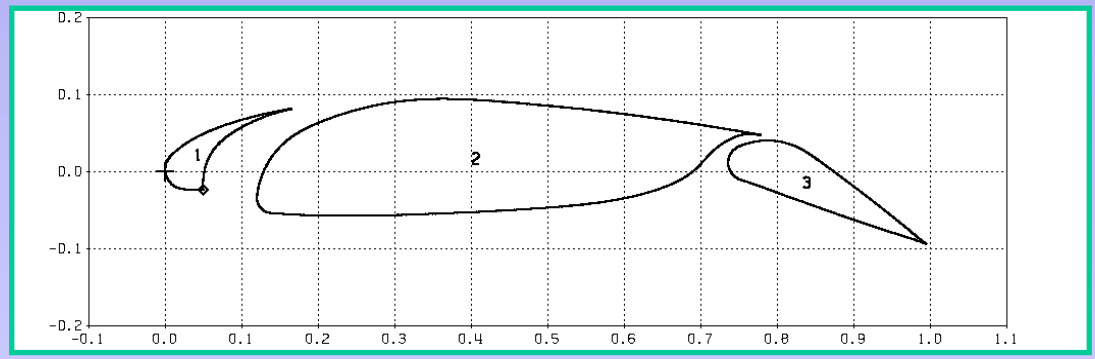

HIGHT LIFT DEVICES

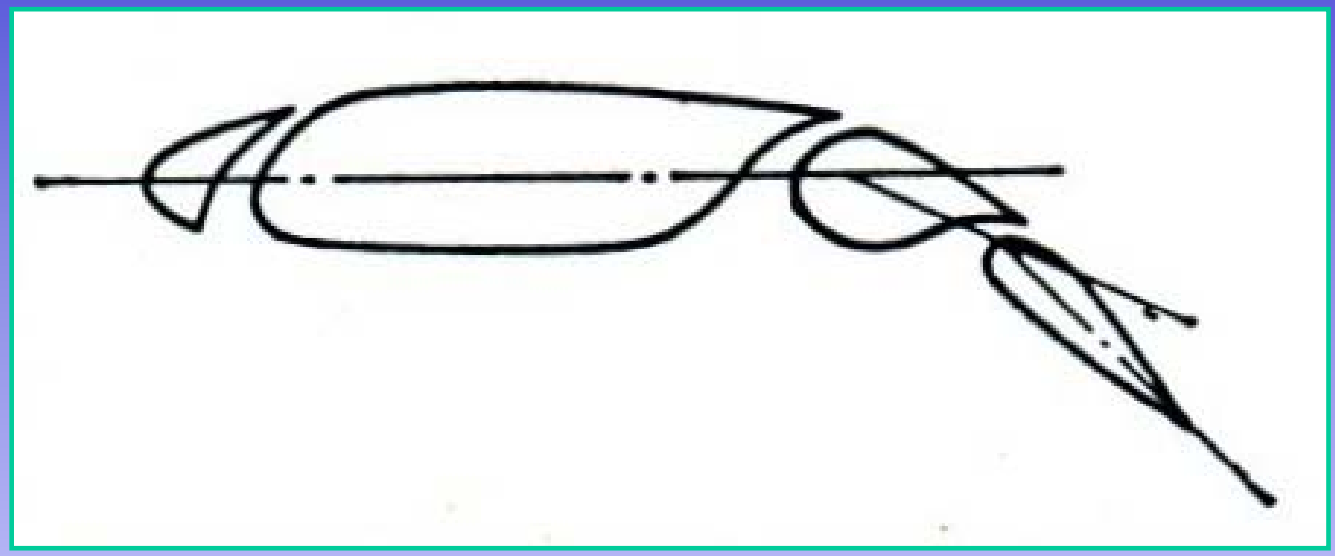

HIGHT LIFT DEVICES

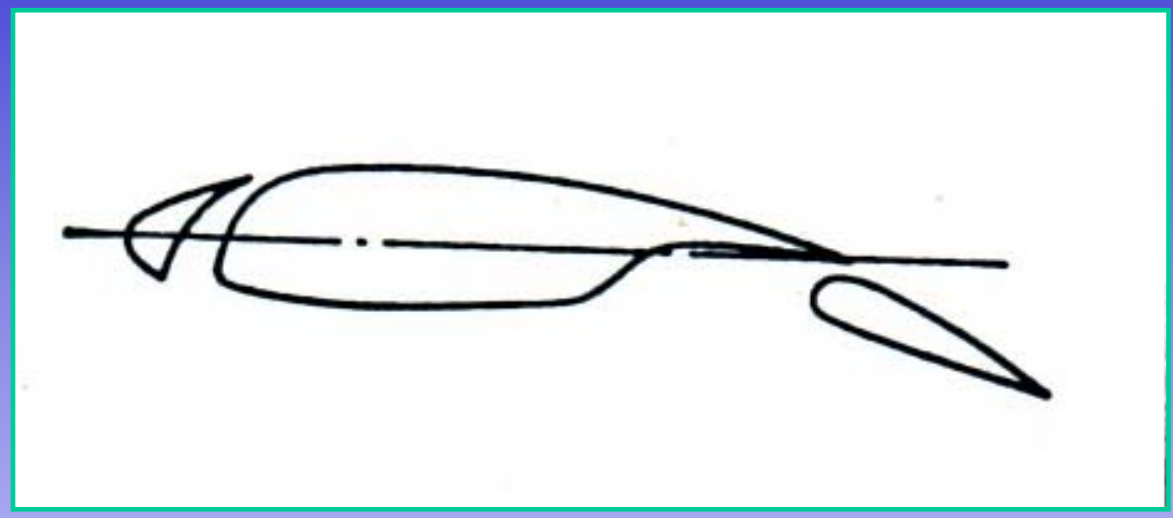

HIGHT LIFT DEVICES

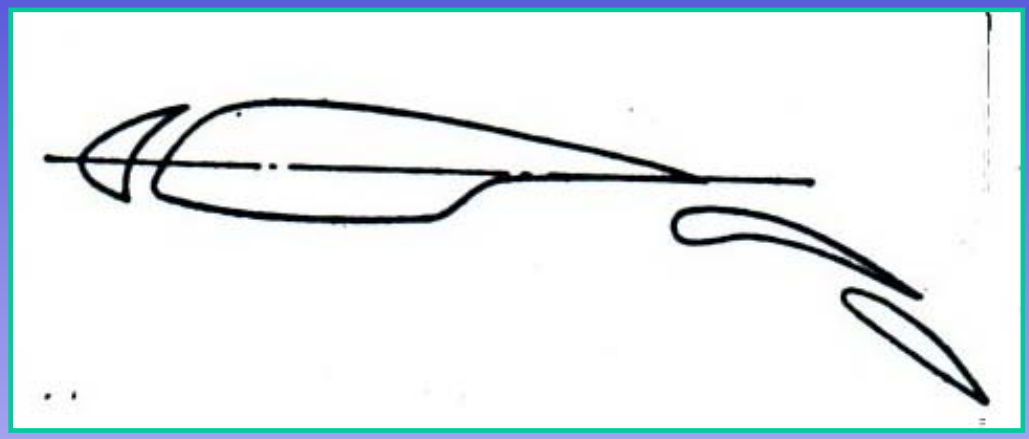

HIGHT LIFT DEVICES

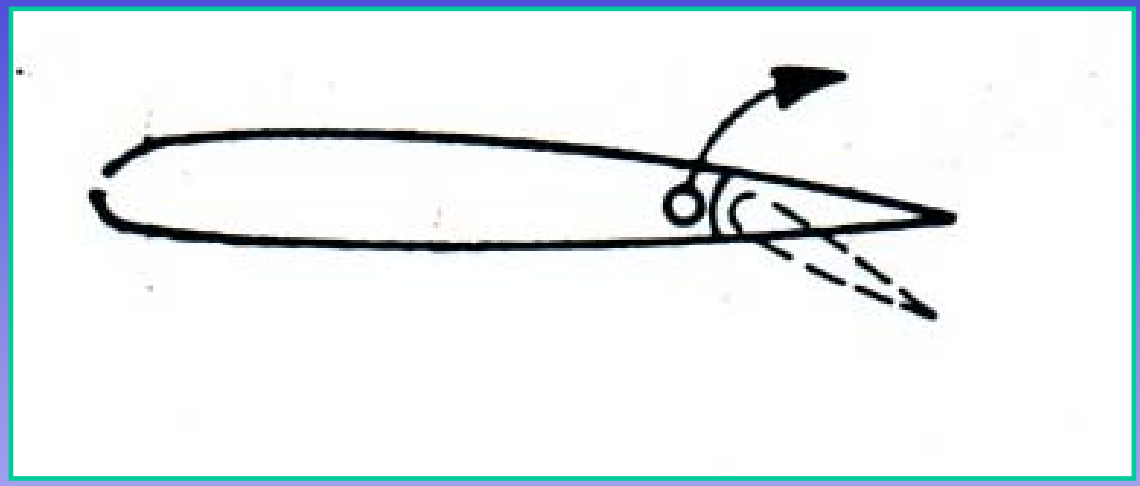

HIGHT LIFT DEVICES

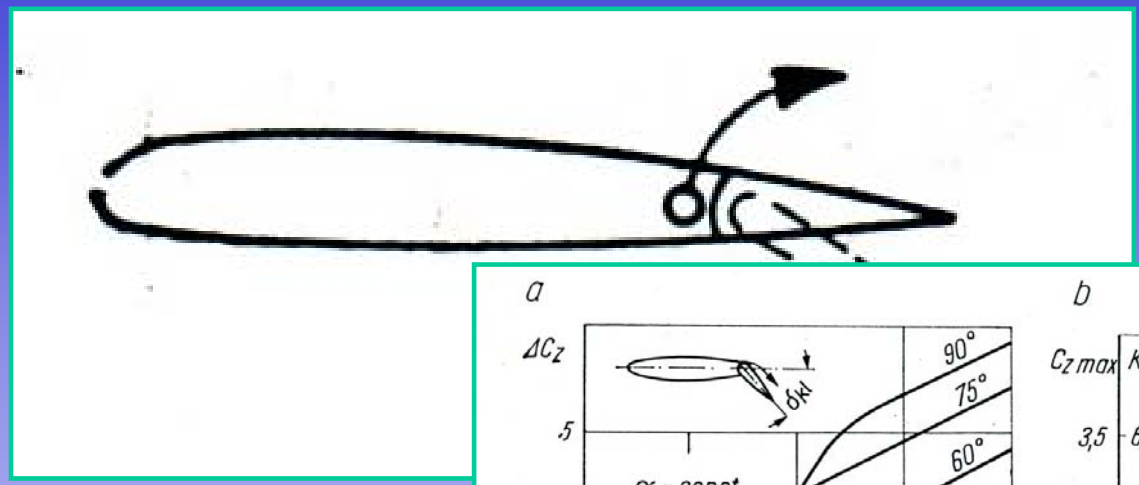

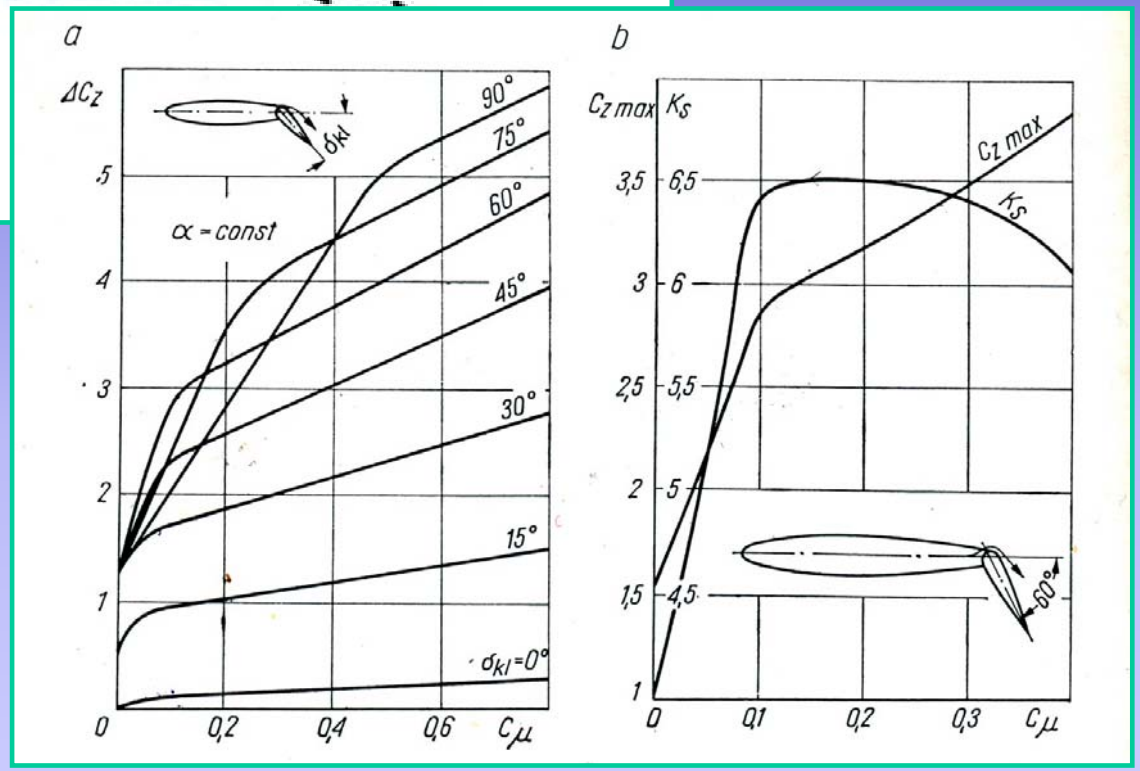

HIGHT LIFT DEVICES

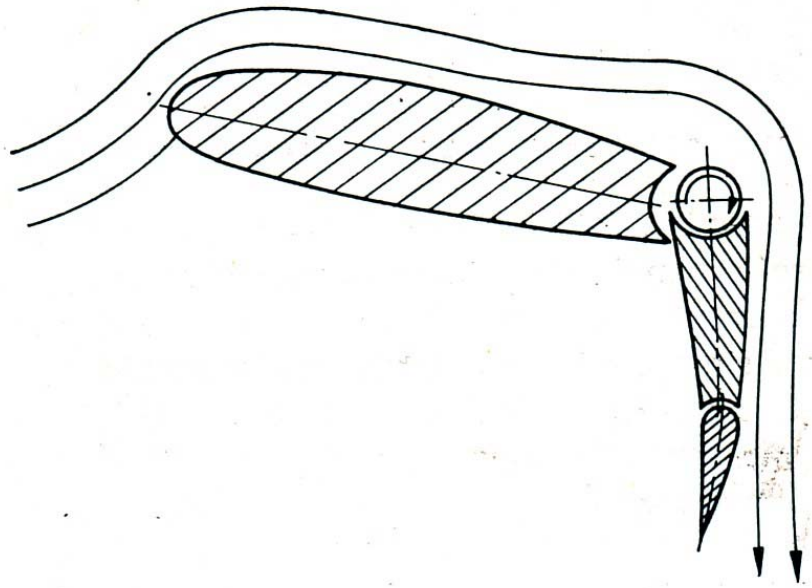

Rys. 9.22. Klapa samolotu NORTH AMERICAN OV-10A „Bronco"

HIGHT LIFT DEVICES

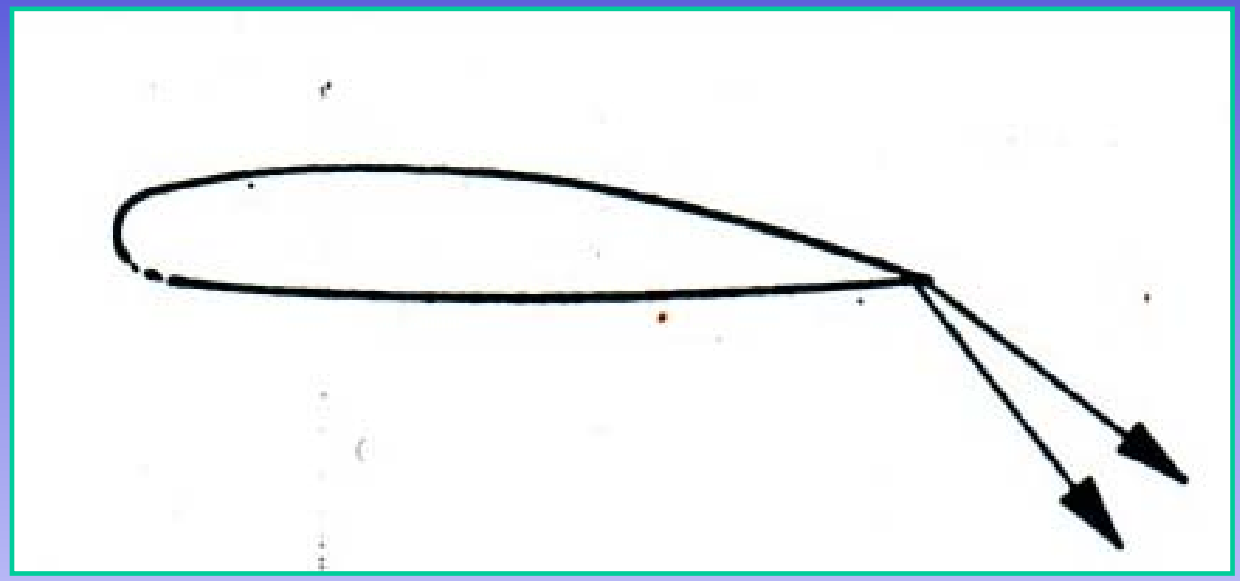

Thin Airfoil Theory (Glauert)

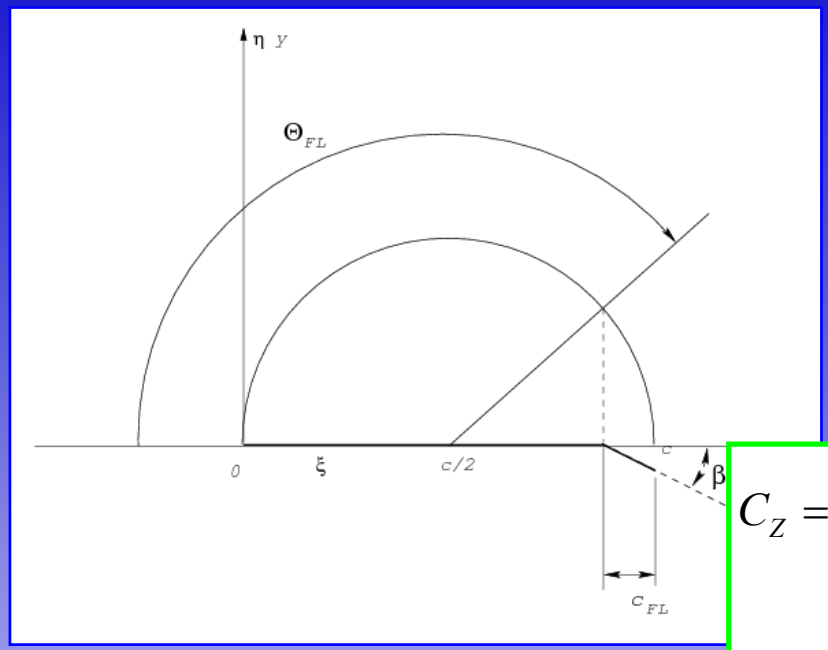

$$C_Z = 2\pi \cdot \left(A_0 + \frac{1}{2} A_1 \right) =$$

$$2\pi \cdot \Big(\underbrace{\alpha + \left(1 - \frac{\Theta_{FL} - \sin(\Theta_{FL})}{\pi} \right) \cdot \beta_{FL}}_{-\alpha_0} \Big)$$

$$\underbrace{2\pi \cdot \alpha + 2\pi \left(1 - \frac{\Theta_{FL} - \sin(\Theta_{FL})}{\pi} \right) \cdot \beta_{FL}}_{C_{Z_0}}$$

HIGHT LIFT DEVICES

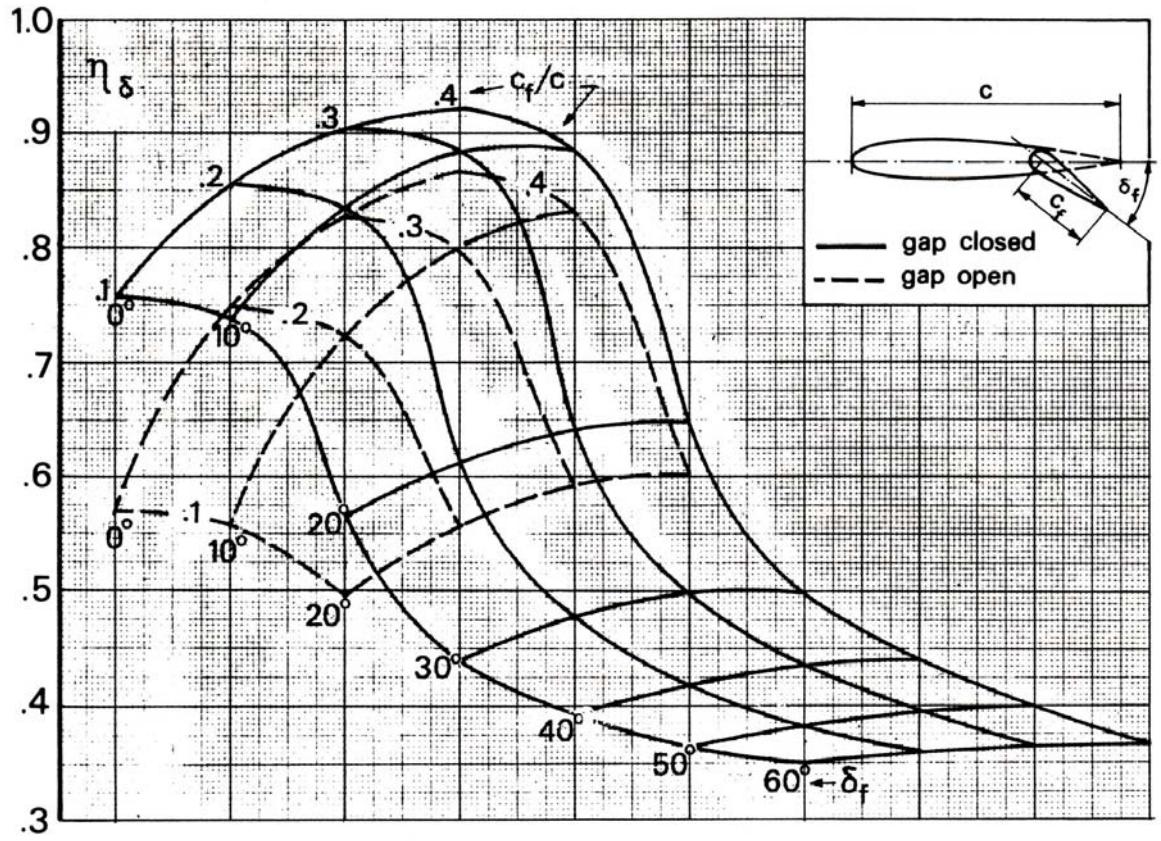

Fig. G-4. Lift effectiveness factor for plain flaps (derived from experimental data in the USAF Datcom, Table 6.1.1.1.-A and Ref. G-64)

HIGHT LIFT DEVICES

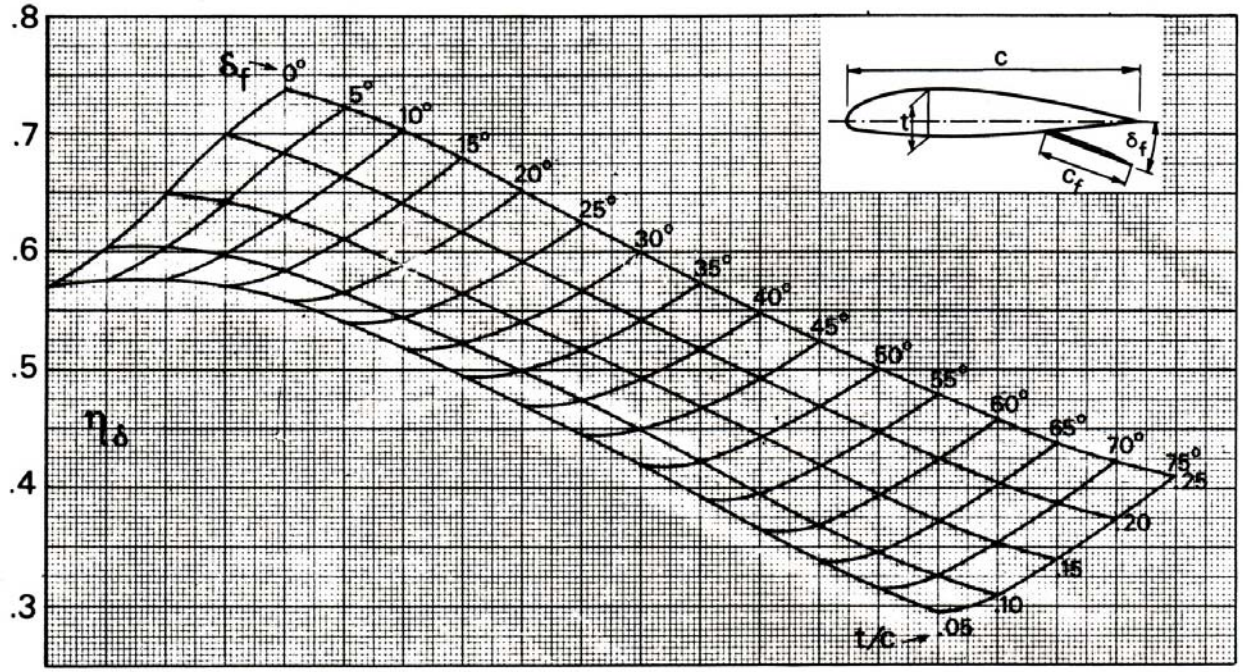

Fig. G-3. Lift-effectiveness factor for split flaps (derived from experimental data in Ref. G-34 and the USAF Datcom, Table 6.1.1.1.-24)

HIGHT LIFT DEVICES

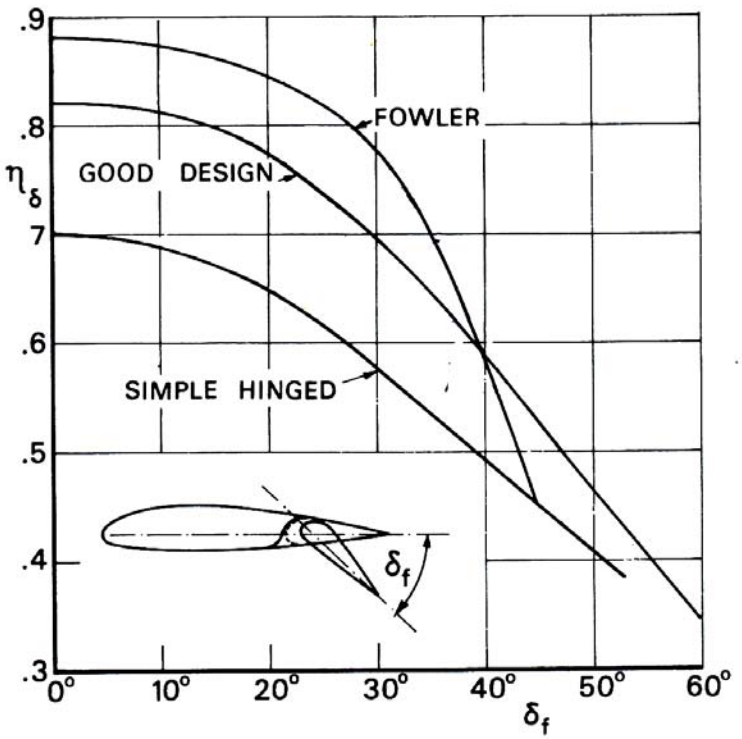

Fig. G-5. Lift effectiveness of single slotted (Fowler) flaps (derived from experimental data in Refs. G-33, G-35, G-37 and G-19)

HIGHT LIFT DEVICES

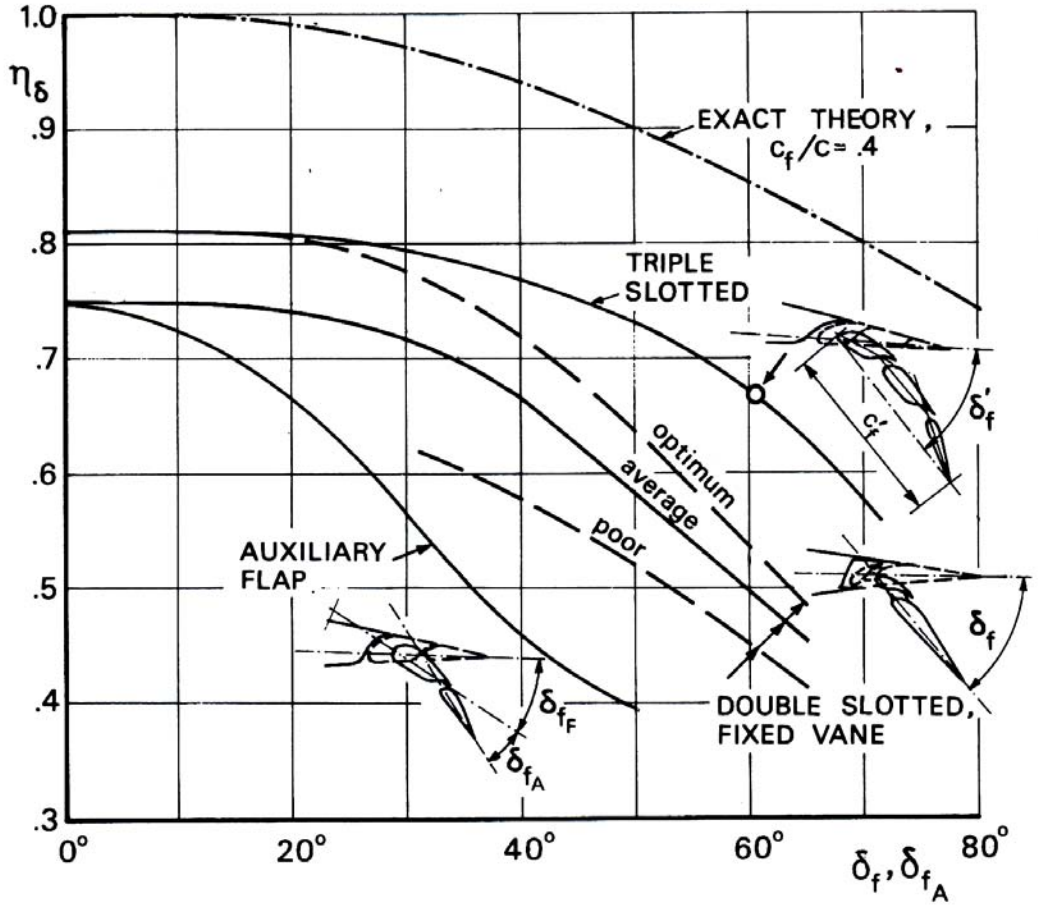

Fig. G-6. Flap effectiveness factor for double and triple slotted flaps (derived from experimental data in Refs. G-3, G-19, G-29, G-39, G-44 and G-48)

HIGHT LIFT DEVICES